Geochemistry of the dissolved loads of rivers during high-flow season in Southeast Coastal Region, China: Anthropogenic impact on chemical weathering and carbon sequestration

Wenjing Liu[1,2,3,4], Zhifang Xu[1,2,3,4*], Huiguo Sun[1,2,3,4], Tong Zhao[1,2,3,4], Chao Shi[1,4], Taoze Liu[5]

[1] Key Laboratory of Cenozoic Geology and Environment, Institute of Geology and Geophysics, Chinese Academy of Sciences, Beijing 100029, China

[2] CAS Center for Excellence in Life and Paleoenvironment, Beijing, 100044, China

[3] Institutions of Earth Science, Chinese Academy of Sciences, Beijing 100029, China

[4] University of Chinese Academy of Sciences, Beijing 100049, China

[5] State Key Laboratory of Environmental Geochemistry, Institute of Geochemistry, Chinese Academy of Sciences, Guiyang, Guizhou 550002, China

* Corresponding author. zfxu@mail.iggcas.ac.cn (Zhifang Xu, Tel: +86 10 82998289)

Abstract:

Southeast coastal region is one of the most developed and populated area in China. Meanwhile, it has been a severe acid rain impacted region for many years. The chemical compositions and carbon isotope ratio of dissolved inorganic carbon ($\delta^{13}C_{DIC}$) of river waters in high flow season were investigated to evaluate the chemical weathering and associated atmospheric CO_2 consumption rates. Mass balance calculation indicated that the dissolved loads of major rivers in the Southeast Coastal Rivers Basin (SECRB) were contributed by atmospheric (14.3%, 6.6-23.4%), anthropogenic (15.7%, 0-41.1%), silicate weathering (39.5%, 17.8-74.0%) and carbonate weathering inputs (30.6%, 3.9-62.0%). The silicate and carbonate chemical weathering rates for these river watersheds were 14.2-35.8 t km^{-2} a^{-1} and 1.8-52.1 t km^{-2} a^{-1}, respectively. The associated mean CO_2 consumption rate by silicate weathering for the whole SECRB were 191×10^3 mol km^{-2} a^{-1}. The chemical and $\delta^{13}C_{DIC}$ evidences indicated that sulfuric and nitric acid (mainly from acid deposition) was significantly involved in chemical weathering of rocks. The calculation showed an overestimation of CO_2 consumption at 0.19×10^{12} g C a^{-1} if sulfuric and nitric acid was ignored, which accounted for about 33.6% of the total CO_2 consumption by silicate weathering in the SECRB. This study quantitatively highlights that the role of acid deposition in chemical weathering, suggesting that anthropogenic impact should be seriously considered in estimation of chemical weathering and associated CO_2 consumption.

Keywords: Southeast Coastal Rivers Basin; Chemical weathering; CO_2 consumption;

35 acid deposition;

36 **1. Introduction**

37 Chemical weathering of rocks is a key process that links geochemical cycling of
38 solid earth to the atmosphere and ocean. It provides nutrients to terrestrial and marine
39 ecosystems and regulates the level of atmospheric CO_2. As a net sink of atmospheric
40 CO_2 on geologic timescales, estimation of silicate chemical weathering rates and the
41 controlling factors are important issues related to long-term global climate change
42 (e.g. Raymo and Ruddiman, 1992; Négrel et al. 1993; Berner and Caldeira, 1997;
43 Gaillardet et al., 1999; Kump et al., 2000; Amiotte-Suchet et al., 2003; Oliva et al.,
44 2003; Hartmann et al., 2009; Moon et al., 2014). As an important component in the
45 Earth's Critical Zone (U.S. Nat. Res. Council Comm., 2001), river serves as an
46 integrator of various natural and anthropogenic processes and products in a basin, and
47 a carrier transporting the weathering products from continent to ocean. Therefore, the
48 chemical compositions of river are widely used to evaluate chemical weathering and
49 associated CO_2 consumption rates at catchment and/or continental scale, and examine
50 their controlling factors (e.g., Edmond et al., 1995; Gislason et al., 1996; Galy and
51 France-Lanord, 1999; Huh, 2003; Millot et al., 2002, 2003; Oliva et al., 2003; West et
52 al., 2005; Moon et al., 2007; Noh et al., 2009; Shin et al., 2011; Calmels et al., 2011;
53 Li, S., et al. 2014).

54 With the intensification of human activities, human perturbations to river basins
55 have increased in frequency and magnitude (Raymond et al., 2008; Regnier et al.,
56 2013; Li and Bush, 2015). It is important to understand how such perturbations

57 function on the current weathering systems and to predict how they will affect the
58 Critical Zone of the future (Brantley and Lebedeva, 2011). In addition to CO_2, other
59 sources of acidity (such as sulfuric, nitric and organic acids) can also produce protons.
60 These protons react with carbonate and silicate minerals, thus enhance rock chemical
61 weathering rate and flux compared with only considering protons deriving from CO_2
62 dissolution (Calmels et al., 2007; Xu and Liu, 2010). The effect of other sourced
63 proton (especially H^+ induced by SO_2 and NO_X coming from anthropogenic activities)
64 on chemical weathering is documented to be an important mechanism modifying
65 atmospheric CO_2 consumption by rock weathering (Galy and France-Lanord, 1999;
66 Semhi, et al., 2000; Spence and Telmer, 2005; Xu and Liu, 2007; Perrin et al., 2008;
67 Gandois et al., 2011). Anthropogenic emissions of SO_2 was projected to provide 3 to 5
68 times greater H_2SO_4 to the continental surface than the pyrite oxidation originated
69 H_2SO_4 (Lerman et al., 2007). Therefore, increasing acid precipitation due to intense
70 human activities nowadays could make this mechanism more prominently.

71 The role of acid precipitation on the chemical weathering and CO_2 consumption
72 has been investigated in some river catchments (Amiotte-Suchet et al., 1995; Probst et
73 al., 2000; Vries et al., 2003; Lerman et al., 2007; Xu and Liu, 2010). It has been
74 documented that silicate rocks were more easily disturbed by acid precipitation during
75 their weathering and soil leaching processes, because of their low buffeting capacity
76 (Reuss et al., 1987; Amiotte-Suchet et al., 1995). The disturbance could be intensive
77 and cause a decrease of CO_2 consumption about 73% by weathering due to acid
78 precipitation in the Strengbach catchment (Vosges Mountains, France), where is

79 dominated by crystalline rocks (Amiotte-Suchet et al., 1995). This highlights the
80 importance of exploring anthropogenic impact on chemical weathering and CO_2
81 consumption under different background (e.g. lithology, climate, human activity
82 intensity, and basin scale) for better constraining and estimation of acid precipitation
83 effect on rock weathering. Asia, especially East Asia, is one of the world's major
84 sulfur and nitrogen emissions areas. However, the effect of acid precipitation on
85 silicate weathering and associated CO_2 consumption was not well evaluated in this
86 area, especially lack of quantitative studies.

87 Acid precipitation affected about 30% of the territory of China (Fig. 1), and the
88 seriously areas are mainly located in the east, the south and the center of China, where
89 over 70% of cities were suffering from acid rain (Zhang et al., 2007a; State
90 Environmental Protection Administration of China, 2009). Southeast coastal region of
91 China is one of the most developed and populated areas of this country, dominated by
92 Mesozoic magmatic rocks (mainly granite and volcanic rocks) in lithology.
93 Meanwhile, the southeast coastal area has become one of the three major acid rain
94 areas in China since the beginning of the 1990s (Larssen et al., 1999). It is seriously
95 impacted by acid rain, with a volume-weighted mean value of pH lower than 4.5 for
96 many years (Wang et al., 2000; Larssen and Carmichael, 2000; Zhao, 2004; Han et al.,
97 2006; Larssen et al., 2006; Zhang et al., 2007a; Huang et al., 2008; Xu et al., 2011).
98 Therefore, it is an ideal area for evaluating silicate weathering and the effect of acid
99 rain. In the previous work, we have recognized and discussed the importance of
100 sulfuric acid on the rock weathering and associated CO_2 consumption in the Qiantang

river basin in this area (Liu et al., 2016). However, it is difficult to infer the anthropogenic impact on chemical weathering and CO_2 consumption in the whole southeast coastal area from the case study of the single river basin, because of the variations on lithology, basin scale, runoff and anthropogenic background in the large acid deposition affected area. In this study, the chemical and carbon isotope composition of rivers in this area were first systematically investigated, in order to: (i) decipher the different sources of solutes and to quantify their contributions to the dissolved loads; (ii) calculate silicate weathering and associated CO_2 consumption rates; (iii) evaluate the effects of acid deposition on rock weathering and CO_2 consumption flux in the whole southeast coastal rivers basin.

2. Natural setting of study area

Southeast coastal region of China, where the landscape is dominated by mountainous and hilly terrain, lacks the conditions for developing large rivers. The rivers in this region are dominantly small and medium-sized due to the topographic limitation. Only 5 rivers in this region have length over 200 km and the drainage area over 10,000 km^2, and they are in turn from north to south: the Qiantangjiang (Qiantang) and the Oujiang (Ou) in Zhejiang province, the Minjiang (Min) and the Jiulongjiang (Jiulong) in Fujian province and the Hanjiang (Han) in Guangdong province (Fig. 1). Rivers in this region generally flow eastward or southward and finally inject into the East China Sea or the South China Sea (Fig. 1), and they are collectively named as 'Southeast Coastal Rivers' (SECRs).

The Southeast Coastal Rivers Basin (SECRB) belongs to the warm and humid

123 subtropical oceanic monsoon climate. The mean annual temperature and precipitation
124 are 17-21℃ and 1400-2000 mm, respectively. The precipitation mainly happens
125 during May to September, and the minimum and maximum temperature often occurs
126 in January and July. This area is one of the most developed areas in China, with a
127 population more than 190 million (mean density of ~470 individuals/km^2), but the
128 population mainly concentrated in the coastal urban areas. The vegetation coverage of
129 these river basins is more than 60%, mainly subtropical evergreen-deciduous
130 broadleaf forest and mostly distributing in mountains area. Cultivated land, and
131 industries and cities are mainly located in the plain areas and lower reach of these
132 rivers.

133 Geologically, three regional-scale fault zones are distributed across the SECRB
134 region (Fig. 1). They are the sub-EW-trending Shaoxing-Jiangshan fault zone, the
135 NE-trending Zhenghe-Dapu fault zone, and the NE-trending Changle-Nanao fault
136 zone (Shu et al., 2009). These fault zones dominate the direction of the mountains
137 ridgelines and drainages, as well as the formation of the basins and bay. The Zhenghe-
138 Dapu fault zone is a boundary line of Caledonian uplift belt and Hercynian-Indosinian
139 depression zone. Mesozoic magmatic rocks are widespread in the southeast coastal
140 region with a total outcrop area at about 240,000 km^2. Over 90% of the Mesozoic
141 magmatic rocks are granitoids (granites and rhyolites) and their volcanic counterpart
142 with minor existence of basalts (Zhou et al., 2000, 2006; Bai et al., 2014). These crust-
143 derived granitic rocks are mainly formed in the Yanshanian stage, and may have been
144 related to multiple collision events between Cathaysia and Yangtze blocks and Pacific

145 plate (Zhou and Li, 2000; Xu et al., 2016). Among the major river basins, the
146 proportions of magmatic rocks outcrop are about 36% in the Qiantang catchment,
147 over 80% in the Ou, the Jiaoxi and the Jin catchments, and around 60% in the Min,
148 the Jiulong, the Han and the Rong catchments (Shi, 2014). The overlying Quaternary
149 sediment in this area is composed of brown-yellow siltstones but is rarely developed.
150 The oldest basement complex is composed of metamorphic rocks of greenschist and
151 amphibolite facies. Sedimentary rocks categories into two types, one is mainly
152 composed by red clastic rocks which cover more than 40,000 km^2 in the area; the
153 other occurs as interlayers within volcanic formations, including varicolored
154 mudstones and sandstones. They are mainly distributed on the west of Zhenghe-Dapu
155 fault zone (FJBGRM, 1985; ZJBGMR, 1989; Shu et al., 2009).

156 **3. Sampling and analytical method**

157 A total of 121 water samples were collected from mainstream and tributaries of
158 the major rivers in the SECRB from July 8th to 31 of 2010 in the high-flow period
159 (sample number and locations are shown in Fig. 1). For the river low reach samples,
160 the sampling sites were selected as far as possible from the tidal impacted area and the
161 sampling were conducted during low tide period (based on the daily tidal time,
162 http://ocean.cnss.com.cn/) in the sampling day. Besides, the salinity of the waters
163 were checked by salinometer (WS202, China) before sampling in the field. In
164 addition, water chemistry data were double checked to make sure that the river
165 samples were not contaminated by seawater. 2-L water samples were collected in the
166 middle channel of the river from bridges or ferries, or directly from the center of some

167 shallow streams in the source area. The lower reaches sampling sites were selected
168 distant away from the estuary to avoid the influence of seawater. Temperature (T), pH
169 and electrical conductivity (EC) were measured in the field with a portable EC/pH
170 meter (YSI-6920, USA). All of the water samples for chemical analysis were filtered
171 in field through 0.22 μm Millipore membrane filter, and the first portion of the
172 filtration was discarded to wash the membrane and filter. One portion filtrate were
173 stored directly in HDPE bottles for anion analysis and another were acidified to pH <
174 2 with 6 M double sub-boiling distilled HNO_3 for cation analysis. All containers were
175 previously washed with high-purity HCl and rinsed with Milli-Q 18.2 MΩ water.
176 Alkalinity was determined by phenolphthalein and methyl orange end point titration with
177 dilute HCl within 12 h after sampling. The HCl consumption volumes for phenolphthalein
178 and methyl orange end point titration were used to calculate the HCO_3^-. Cations (Na^+, K^+,
179 Ca^{2+} and Mg^{2+}) were determined using Inductively Coupled Plasma Atomic Emission
180 Spectrometer (ICP-AES) (IRIS Intrepid II XSP, USA). Anions (Cl^-, F^-, NO_3^- and
181 SO_4^{2-}) were analyzed by ionic chromatography (IC) (Dionex Corporation, USA).
182 Dissolved silica was determined by spectrophotometry using the molybdate blue
183 method. Reagent and procedural blanks were measured in parallel to the sample
184 treatment, and calibration curve was evaluated by quality control standards before,
185 during and after the analyses of each batch of samples. Measurement reproducibility
186 was determined by duplicated sample and standards, which showed ±3% precision for
187 the cations and ±5% for the anions.
188 River water samples for carbon isotopic ratio ($\delta^{13}C$) of dissolved inorganic

carbon (DIC) measurements were collected in 150 ml glass bottles with air-tight caps and preserved with $HgCl_2$ to prevent biological activity. The samples were kept refrigerated until analysis. For the $\delta^{13}C$ measurements, the filtered samples were injected into glass bottles with phosphoric acid. The CO_2 was then extracted and cryogenically purified using a high vacuum line. $\delta^{13}C$ isotopic ratios were analyzed on Finnigen MAT-252 stable isotope mass spectrometer at the State Key Laboratory of Environmental Geochemistry, Chinese Academy of Sciences. The results are expressed with reference to VPDB, as follows:

$$\delta^{13}C = [(({}^{13}C/{}^{12}C)_{sample} / ({}^{13}C/{}^{12}C)_{standard}) - 1] \times 1000 \quad (1)$$

The $\delta^{13}C$ measurement has an overall precision of 0.1‰. A number of duplicate samples were measured and the results show that the differences were less than the range of measurement accuracy.

4. Results

The major parameter and ion concentrations of samples are given in Table 1. The pH values of water samples ranged from 6.50 to 8.24, with an average of 7.23. Total dissolved solids (TDS) of water samples varied from 35.3 to 205 mg l^{-1}, with an average of 75.2 mg l^{-1}. Compared with the major rivers in China, the average TDS was significantly lower than the Changjiang (224 mg l^{-1}, Chetelat et al., 2008) , the Huanghe (557 mg l^{-1}, Fan et al., 2014) and the Zhujiang (190 mg l^{-1}, Zhang et al., 2007b). However, the average TDS was comparable to the rivers draining silicate rock dominated areas, e.g. the upper Ganjiang in Ganzhou, south China (63 mg l^{-1}, Ji and Jiang, 2012), the Amur in north China (70 mg l^{-1}, Moon et al., 2009), the Xishui in

211 Hubei, central China (101 mg l^{-1}, Wu et al., 2013), and north Han river in South Korea
212 (75.5 mg l^{-1}, Ryu et al., 2008). Among the major rivers in the SECRB, the Qiantang
213 had the highest TDS value (averaging at 121 mg l^{-1}), and the Ou had the lowest TDS
214 value (averaging at 48.8 mg l^{-1}).

215 Major ion compositions are shown in the cation and anion ternary diagrams (Fig.
216 2a and b). In comparison with rivers (e.g. the Wujiang and Xijiang) draining
217 carbonate rocks dominated area (Han and Liu, 2004; Xu and Liu, 2010), these rivers
218 in the SECRB had distinctly higher proportions of Na^+, K^+, and dissolved SiO_2. As
219 shown in the Fig. 2, most samples had high Na^+ and K^+ proportions, with an average
220 more than 50% (in μmol l^{-1}) of the total cations, except for samples from the
221 Qiantang. The concentrations of Na^+ and K^+ ranged from 43.5 to 555 μmol l^{-1} and
222 42.9 to 233 μmol l^{-1}, with average values of 152 and 98 μmol l^{-1}, respectively. The
223 concentrations of dissolved SiO_2 ranged from 98.5 to 370 μmol l^{-1}, with an average of
224 212 μmol l^{-1}. Ca^{2+} and Mg^{2+} accounted for about 38% and 11.6% of the total cation
225 concentrations. HCO_3^- was the dominant anion with concentrations ranging from 139
226 to 1822 μmol l^{-1}. On average, it comprised 60.6% (36-84.6%) of total anions on a
227 molar basis, followed by SO_4^{2-} (14.6%), Cl^- (13.1%) and NO_3^- (11.8%). The major
228 ionic compositions indicate that water chemistry of these rivers in the SECRB is
229 controlled by silicate weathering. Meanwhile, it is also influenced by carbonate
230 weathering, especially in the Qiantang catchment.

231 The $\delta^{13}C$ of dissolved inorganic carbon in the rivers of the SECRB are also given
232 in Table 1. The $\delta^{13}C$ of the water samples showed a wide range, from -11.0‰ to -

24.3‰ (average -19.4‰), and with a majority of samples falling between -15 and -23‰. The values are similar to rivers draining Deccan Traps (Das et al., 2005).

5. Discussion

The dissolved solids in river water are commonly from atmospheric and anthropogenic inputs and weathering of rocks within the drainage basin. It is necessary to quantify the contribution of different sources to the dissolved loads before deriving chemical weathering rates and associated CO_2 consumption.

5.1 Atmospheric and anthropogenic inputs

To evaluate atmospheric inputs to river waters, chloride is the most common used reference. Generally, water samples that have the lowest Cl^- concentrations are employed to correct the proportion of atmospheric inputs in a river system (Négrel et al., 1993; Gaillardet et al., 1997; Viers et al., 2001; Xu and Liu, 2007). In pristine areas, the concentration of Cl^- in river water is assumed to be entirely derived from the atmosphere, provided that the contribution of evaporites is negligible (e.g. Stallard and Edmond, 1981; Négrel et al., 1993). In the SECRB, the lowest Cl^- concentration was mainly found in the headwater of each river. According to the geologic setting, no salt-bearing rocks was found in these headwater area (FJBGRM, 1985; ZJBGMR, 1989). In addition, these areas are mainly mountainous and sparsely populated. Therefore, we assumed that the lowest Cl^- concentration of samples from the headwater of each major river came entirely from atmosphere.

The proportion of atmosphere-derived ions in the river waters can then be calculated by using the element/Cl ratios of the rain. Chemical compositions of rain in

255 the studied area have been reported at different sites, including Hangzhou, Jinhua,
256 Nanping, Fuzhou and Xiamen (Zhao, 2004; Zhang et al., 2007a; Huang et al., 2008;
257 Cheng et al., 2011; Xu et al., 2011) (Fig. 1). The volume-weighted mean
258 concentration of ions and Cl-normalized molar ratios are compiled in Table 2.
259 According to this procedure, 6.6-23.4% (averaging 14.3%) of total dissolved cations
260 in the major rivers of the SECRB originated from rain. Among the anions, SO_4^{2-} and
261 NO_3^- in the rivers are mainly from the atmospheric input, averaging at 73.2% for
262 SO_4^{2-} and 75.8% for NO_3^-, respectively.

263 As one of the most developed and populated areas in China, the chemistry of
264 river waters in the SECRB could be significantly impacted by anthropogenic inputs.
265 Cl^-, NO_3^- and SO_4^{2-} are commonly associated with anthropogenic sources and have
266 been used as tracers of anthropogenic inputs in watershed. High concentrations of Cl^-,
267 NO_3^- and SO_4^{2-} can be found at the lower reaches of rivers in the SECRB, and an
268 obvious increase after flowing through plain areas and cities. This tendency indicates
269 that river water chemistry is affected by anthropogenic inputs while passing through
270 the catchments. After correcting for the atmospheric contribution to river waters, the
271 following assumption is needed to quantitatively estimate the contributions of
272 anthropogenic inputs. That is, Cl^- originates from only atmospheric and anthropogenic
273 inputs, the excess of atmospheric Cl^- is regarded to present anthropogenic inputs and
274 balanced by Na^+.

275 *5.2 Chemical weathering inputs*

276 Water samples were displayed on a plot of Na-normalized molar ratios (Fig. 3).

277 The values of the world's large rivers (Gaillardet et al. 1999) are also shown in the
278 figure. A best correlations between elemental ratios were observed for Ca^{2+}/Na^{+} vs.
279 Mg^{2+}/Na^{+} (R^2 = 0.95, n = 120) and Ca^{2+}/Na^{+} vs. HCO_3^{-}/Na^{+} (R^2 = 0.98, n = 120). The
280 samples cluster on a mixing line mainly between silicate and carbonate end-members,
281 closer to the silicate end-member, and with little evaporite contribution. This
282 corresponds with the distribution of rock types in the SECRB. In addition, all water
283 samples have equivalent ratios of $(Na^{+}+K^{+})/Cl^{-}$ larger than one, indicating silicate
284 weathering as the source of Na^{+} and K^{+} rather than chloride evaporites dissolution.
285 The geochemical characteristics of the silicate and carbonate end-members can
286 be deduced from the correlations between elemental ratios and referred to literature
287 data for catchments with well-constrained lithology. After correction for atmospheric
288 inputs, the Ca^{2+}/Na^{+}, Mg^{2+}/Na^{+} and HCO_3^{-}/Na^{+} of the river samples ranged from 0.31
289 to 30, 0.16 to 6.7, and 1.1 to 64.2, respectively. According to the geological setting
290 (Fig. 1), there are some small rivers draining purely silicate areas in the SECRs
291 drainage basins. Based on the elemental ratios of these rivers, we assigned the silicate
292 end-member for this study as Ca^{2+}/Na^{+}=0.41±0.10, Mg^{2+}/Na^{+}=0.20±0.03 and HCO_3^{-}
293 $/Na^{+}$=1.7±0.6. The ratio of $(Ca^{2+}+Mg^{2+})/Na^{+}$ for silicate end-member was 0.61±0.13,
294 which is close to the silicate end-member of world rivers ($(Ca^{2+}+Mg^{2+})/Na^{+}$ =
295 0.59±0.17, Gaillardet et al., 1999). Moreover, previous researches have documented
296 the chemical composition of rivers, such as the Amur and the Songhuajiang in North
297 China, the Xishui in the lower reaches of the Changjiang, and major rivers in South
298 Korea (Moon et al., 2009; Liu et al., 2013; Wu et al., 2013; Ryu et al., 2008; Shin et

al., 2011). These river basins has similar lithological setting with the study area, we could further validate the composition of silicate end-member with their results. Ca^{2+}/Na^{+} and Mg^{2+}/Na^{+} ratios of silicate end-member were reported for the Amur (0.36 and 0.22), the Songhuajiang (0.44±0.23 and 0.16), the Xishui (0.6±0.4 and 0.32±0.18), the Han (0.55 and 0.21) and six major rivers in South Korea (0.48 and 0.20) in the studies above, well bracketing our estimation for silicate end-member.

Whereas, some samples show high concentrations of Ca^{2+}, Mg^{2+} and HCO_3^-, indicating the contribution of carbonate weathering. The samples collected in the upper reaches (Sample 12 and 13) of the Qiantang fall close to the carbonate end-member documented for world's large rivers (Gaillardet et al., 1999). In the present study, Ca^{2+}/Na^{+} ratio of 0.41±0.10 and Mg^{2+}/Na^{+} ratio of 0.20±0.03 for silicate end-member are used to calculate the contribution of Ca^{2+} and Mg^{2+} from silicate weathering. Finally, residual Ca^{2+} and Mg^{2+} are apportioned to carbonate weathering.

5.3 Chemical weathering rate in the SECRBs

Based on the above assumption, a forward model is employed to quantify the relative contribution of the different sources to the rivers of the SECRB in this study. (e.g. Galy and France-Lanord, 1999; Moon et al., 2007; Xu and Liu, 2007; 2010; Liu et al., 2013). The calculated contributions of different reservoir to the total cationic loads for major rivers and their main tributaries in the SECRB are presented in Fig. 4. On average, the dissolved cationic loads of the rivers in the study area originate dominantly from silicate weathering, which accounts for 39.5% (17.8-74.0%) of the total cationic loads in molar unit. Carbonate weathering and anthropogenic inputs

account for 30.6% (3.9-62.0%) and 15.7% (0-41.1%), respectively. Contributions from silicate weathering are high in the Ou (55.6%), the Huotong (54.5%), the Ao (48.3%) and the Min (48.3%) river catchments, which dominated by granitic and volcanic bedrocks. In contrast, high contribution from carbonate weathering is observed in the Qiantang (54.0%), the Jin (52.2%) and the Jiulong (44.8%) river catchments. The results manifest the lithology control on river solutes of drainage basin.

The chemical weathering rate of rocks is estimated by the mass budget, basin area and annual discharge (data from the Annual Hydrological Report P. R. China, 2010, Table 3), expressed in ton km^{-2} a^{-1}. The silicate weathering rate (SWR) is calculated using major cationic concentrations from silicate weathering and assuming that all dissolved SiO_2 is derived from silicate weathering (Xu and Liu, 2010), as the equation below:

$$SWR = ([Na]_{sil} + [K]_{sil} + [Ca]_{sil} + [Mg]_{sil} + [SiO_2]_{riv}) \times discharge/area \quad (2)$$

The assumption about Si could lead to overestimation of the silicate weathering rate, as part of silica may come from dissolution of biogenic sources rather than the weathering of silicate minerals (Millot et al., 2003; Shin et al., 2011). Thus, the cationic silicate weathering rates (Cat_{sil}) were also calculated.

The carbonate weathering rate (CWR) is calculated based on the sum of Ca^{2+}, Mg^{2+} and HCO_3^- from carbonate weathering, with half of the HCO_3^- coming from carbonate weathering being derived from the atmosphere CO_2, as the equation below:

$$CWR = ([Ca]_{carb} + [Mg]_{carb} + 1/2[HCO_3]_{carb}) \times discharge/area \quad (3)$$

The chemical weathering rate and flux are calculated for major rivers and their main tributaries in the SECRB, and the results are shown in Table 3. Silicate and carbonate weathering fluxes of these rivers (SWF and CWF) range from 0.02 $\times 10^6$ t a^{-1} to 1.80×10^6 t a^{-1}, and from 0.004×10^6 t a^{-1} to 1.74×10^6 t a^{-1}, respectively. Among the rivers, the Min has the highest silicate weathering flux, and the Qiantang has the highest carbonate weathering flux. On the whole SECRB scale, 3.95×10^6 t a^{-1} and 4.09×10^6 t a^{-1} of dissolved solids originating from silicate and carbonate weathering, respectively, are transported into the East and South China Sea by rivers in this region. Compared with the largest three river basins (the Changjiang, the Huanghe and the Xijiang) in China, the flux of silicate weathering calculated for the SECRB is lower than the Changjiang (9.5×10^6 t a^{-1}, Gaillardet et al. 1999), but higher than the Huanghe (1.52×10^6 t a^{-1}, Fan et al., 2014) and the Xijiang (2.62×10^6 t a^{-1}, Xu and Liu, 2010).

The silicate and carbonate chemical weathering rates for these river watersheds were 14.2-35.8 t km^{-2} a^{-1} and 1.8-52.1 t km^{-2} a^{-1}, respectively. The total rock weathering rate (TWR) for the whole SECRB is 48.1 ton km^{-2} a^{-1}, higher than the world average (24 ton km^{-2} a^{-1}, Gaillardet et al., 1999). The cationic silicate weathering rates (Cat_{sil}) ranges from 4.7 to 12.0 ton km^{-2} a^{-1} for the river watersheds in the SECRB, averaging at 7.8 ton km^{-2} a^{-1}. Furthermore, a good linear correlation (R^2 = 0.77, n = 28) is observed between the Cat_{sil} and runoff (Fig. 5), indicating silicate weathering rates is controlled by the runoff as documented in previous researches (e.g., Bluth and Kump, 1994; Gaillardet et al., 1999; Millot et al., 2002;

Oliva et al., 2003; Wu et al., 2013; Pepin et al., 2013).

5.4 CO_2 consumption and the role of sulfuric acid

To calculate atmospheric CO_2 consumption by silicate weathering (CSW) and by carbonate weathering (CCW), a charge-balanced state between rock chemical weathering-derived alkalinity and cations was assumed (Roy et al., 1999).

$$[CO_2]_{CSW} = [HCO_3]_{CSW} = [Na]_{sil} + [K]_{sil} + 2[Ca]_{sil} + 2[Mg]_{sil} \quad (4)$$

$$[CO_2]_{CCW} = [HCO_3]_{CCW} = [Ca]_{carb} + [Mg]_{carb} \quad (5)$$

The calculated CO_2 consumption rates by chemical weathering for the rivers in SECRB are shown in Table 3. CO_2 consumption rates by carbonate and silicate weathering are from 17.9 to 530×10^3 mol km^{-2} a^{-1} (averaging at 206×10^3 mol km^{-2} a^{-1}) and from 167 to 460×10^3 mol km^{-2} a^{-1} (averaging at 281×10^3 mol km^{-2} a^{-1}) for major river catchments in the SECRB. The CO_2 consumption rates by silicate weathering in the SECRB are higher than that of major rivers in the world and China, such as the Amazon (174×10^3 mol km^{-2} a^{-1}, Mortatti and Probst, 2003), the Mississippi and the Mackenzie (66.8 and 34.1×10^3 mol km^{-2} a^{-1}, Gaillardet et al., 1999), the Changjiang (112×10^3 mol km^{-2} a^{-1}, Chetelat et al., 2008), the Huanghe (35×10^3 mol km^{-2} a^{-1}, Fan et al., 2014), the Xijiang (154×10^3 mol km^{-2} a^{-1}, Xu and Liu, 2010), the Longchuanjiang (173×10^3 mol km^{-2} a^{-1}, Li et al., 2011) and the Mekong (191×10^3 mol km^{-2} a^{-1}, Li et al., 2014) and three large rivers in eastern Tibet (103-121×10^3 mol km^{-2} a^{-1}, Noh et al., 2009), the Hanjiang in central China (120×10^3 mol km^{-2} a^{-1}, Li et al., 2009) and the Sonhuajiang in north China (66.6×10^3 mol km^{-2} a^{-1}, Liu et al., 2013). The high CO_2 consumption rates by silicate weathering in the SECRB could be

attributed to extensive distribution of silicate rocks, high runoff, humid and hot climatic conditions. The regional fluxes of CO_2 consumption by silicate and carbonate weathering is about 47.9×10^9 mol a^{-1} (0.57×10^{12} g C a^{-1}) and 41.9×10^9 mol a^{-1} (0.50×10^{12} g C a^{-1}) in the whole SECRB.

However, in addition to CO_2, the anthropogenic sourced proton (e.g. H_2SO_4 and HNO_3) is well documented as significant proton providers in rock weathering process (Galy and France-Lanord, 1999; Karim and Veizer, 2000; Yoshimura et al., 2001; Han and Liu, 2004; Spence and Telmer, 2005; Lerman and Wu, 2006; Xu and Liu 2007; 2010; Perrin et al., 2008; Gandois et al., 2011). Sulfuric acid can be generated by natural oxidation of pyrite and anthropogenic emissions of SO_2 from coal combustion and subsequently dissolve carbonate and silicate minerals. The riverine nitrate in a watershed can be derived from atmospheric deposition, synthetic fertilizers, microbial nitrification, sewage and manure, etc. (e.g. Kendall 1998). Although it is difficult to determine the sources of nitrate in river waters, we can at least simply assume that nitrate from acid deposition is one of the providers of protons. The consumption of CO_2 by rock weathering would be overestimated if H_2SO_4 and HNO_3 induced rock weathering was ignored (Spence and Telmer, 2005; Xu and Liu, 2010; Shin et al., 2011; Gandois et al., 2011). Thus, the role of the anthropogenic sourced protons on the chemical weathering is crucial for an accurate estimation of CO_2 consumption by rock weathering.

Rapid economic growth and increased energy command have result in severe air pollution problems in China, indicated by the high levels of mineral acids

409 (predominately sulfuric) observed in precipitation (Lassen and Carmichael, 2000; Pan
410 et al., 2013; Liu et al., 2016). The national SO_2 emissions in 2010 reached to 30.8
411 Tg/year (Lu et al., 2011). Previous study documented that fossil fuel combustion
412 accounts for the dominant sulfur deposition (~77%) in China (Liu et al., 2016). The
413 wet deposition rate of nitrogen peaked over the central and south China, with mean
414 value of 20.2, 18.2 and 25.8 kg N ha^{-1} yr^{-1} in Zhejiang, Fujian and Guangdong
415 province, respectively (Lu and Tian, 2007). Current sulfur and nitrogen depositions in
416 the Southeast coastal region are still among the highest in China (Fang et al., 2013;
417 Cui et al., 2014; Liu et al., 2016).

418 The involvement of protons originating from H_2SO_4 and HNO_3 in the river
419 waters can be verified by the stoichiometry between cations and anions, shown in Fig.
420 6. In the rivers of the SECRB, the sum cations released by silicate and carbonate
421 weathering were not balanced by HCO_3^- only (Fig. 6a), but were almost balanced by
422 the sum of HCO_3^- and SO_4^{2-} and NO_3^- (Fig. 6b). This implies that H_2CO_3 and H_2SO_4
423 and HNO_3 are the potential erosion agents in chemical weathering in the SECRB. The
424 $\delta^{13}C$ values of the water samples showed a wide range, from -11.0‰ to -24.3‰, with
425 an average of -19.4‰. The $\delta^{13}C$ from soil is governed by the relative contribution
426 from C_3 and C_4 plant (Das et al., 2005). The studied areas have subtropical
427 temperatures and humidity, and thus C_3 processes are dominant. The $\delta^{13}C$ of soil CO_2
428 is derived primarily from $\delta^{13}C$ of organic material which typically has a value of -24
429 to -34‰, with an average of -28‰ (Faure, 1986). According to previous studies, the
430 average value for C_3 trees and shrubs are from -24.4 to -30.5‰, and most of them are

lower than -28‰ in south China (Chen et al., 2005; Xiang, 2006; Dou et al., 2013). After accounting for the isotopic effect from diffusion of CO_2 from soil, the resulting $\delta^{13}C$ (from the terrestrial C_3 plant process) should be ~ -25‰ (Cerling et al., 1991). This mean DIC derived from silicate weathering by carbonic acid (100% from soil CO_2) would yield a $\delta^{13}C$ value of -25‰. Carbonate rocks are generally derived from marine system and, typically, have $\delta^{13}C$ value close to zero (Das et al., 2005). Thus, the theoretical $\delta^{13}C$ value of DIC derived from carbonate weathering by carbonic acid (50% from soil CO_2 and 50% from carbonate rocks) is -12.5‰. DIC derived from carbonate weathering by sulfuric acid are all from carbonate rocks, thus the $\delta^{13}C$ of the DIC would be 0‰. Based on these conclusions, sources of riverine DIC from different end-members in the SECRB were plotted in Fig. 7. Most water samples drift away from the three endmember mixing area (carbonate and silicate weathering by carbonic acid and carbonate weathering by sulfuric acid) and towards the silicate weathering by sulfuric and nitric acid area, clearly illustrating the effect of the anthropogenic sourced protons on silicate weathering in the SECRB.

Considering the H_2SO_4 and HNO_3 effect on chemical weathering, CO_2 consumption by silicate weathering can be determined from the equation below (Moon et al., 2007; Ryu et al., 2008; Shin et al., 2011):

$$[CO_2]_{SSW} = [Na]_{sil} + [K]_{sil} + 2[Ca]_{sil} + 2[Mg]_{sil} - \gamma\times[2SO_4+NO_3]_{atmos} \quad (6)$$

Where γ is calculated by $cation_{sil}/(cation_{sil} + cation_{carb})$.

Based on the calculation in section 5.1, SO_4^{2-} and NO_3^- in river waters were mainly derived from atmospheric input. Assuming SO_4^{2-} and NO_3^- in river waters

453 derived from atmospheric input (after correction for sea-salt contribution) are all from
454 acid precipitation, CO_2 consumption rates by silicate weathering (SSW) are estimated
455 between 55×10^3 mol km^{-2} a^{-1} and 286×10^3 mol km^{-2} a^{-1} for major river watersheds in
456 the SECRB. For the whole SECRB, the actual CO_2 consumption rates by silicate is
457 191×10^3 mol km^{-2} a^{-1} when the effect of H_2SO_4 and HNO_3 is considered. The flux of
458 CO_2 consumption is overestimated by 16.1×10^9 mol a^{-1} (0.19×10^{12} g C a^{-1}) due to the
459 involvement of H_2SO_4 and HNO_3 from acid precipitation, accounting for
460 approximately 33.6% of total CO_2 consumption flux by silicate weathering in the
461 SECRB. It highlights the fact that the drawdown of atmospheric CO_2 by silicate
462 weathering can be significantly overestimated if acid deposition is ignored in long-
463 term perspectives. The result is important as it quantitatively shows that
464 anthropogenic activities can significantly affect rock weathering and associated
465 atmospheric CO_2 consumption. The quantification of this effect needs to be well
466 evaluated in Asian and global scale within the current and future human activity
467 background.

468 It is noticeable that the chemical weathering and associated CO_2 consumption
469 rates for the study area were calculated by the river water geochemistry of high-flow
470 season. As a subtropical monsoon climate area, the river water of the southeast coastal
471 rivers is mainly recharged by rain, and the amount of precipitation in high-flow
472 season accounts for more than 70% of the annual precipitation in the area. The
473 processes in low-flow season might be different for some extent. It is worth the
474 further effort to investigate the hydrology and temperature effect on weathering rate

and flux, as well as on the anthropogenic impact evaluation in different climate regime and hydrology season.

6. Conclusions

River waters in the southeast coastal region of China are characterized by high proportions of Na^+, K^+ and dissolved SiO_2, indicating water chemistry of the rivers in the SECRB is mainly controlled by silicate weathering. The dissolved cationic loads of the rivers in the study area originate dominantly from silicate weathering, which accounts for 39.5% (17.8-74.0%) of the total cationic loads. Carbonate weathering, atmospheric and anthropogenic inputs account for 30.6%, 14.3% and 15.7%, respectively. Meanwhile, more than 70% of SO_4^{2-} and NO_3^- in the river waters derived from atmospheric input. The chemical weathering rate of silicates and carbonates for the whole SECRB are estimated to be approximately 23.7 and 24.5 ton km^{-2} a^{-1}. About 8.04×10^6 t a^{-1} of dissolved solids originating from rock weathering are transported into the East and South China Sea by these rivers in the SECRB. With the assumption that all the protons involved in the weathering reaction are provided by carbonic acid, the CO_2 consumption rates by silicate and carbonate weathering are 287 and 251×10^3 mol km^{-2} a^{-1}, respectively. However, both water chemistry and carbon isotope data provide evidence that sulfuric and nitric acid from acid precipitation serves as significant agents during chemical weathering. Considering the effect of sulfuric and nitric acid, the CO_2 consumption rate by silicate weathering for the SECRB are 191×10^3 mol km^{-2} a^{-1}. Therefore, the CO_2 consumption flux would be overestimated by 16.1×10^9 mol a^{-1} (0.19×10^{12} g C a^{-1}) in the SECRB if the effect of

sulfuric and nitric acid is ignored. This work illustrates that anthropogenic disturbance by acid precipitation has profound impact on CO_2 sequestration by rock weathering.

Acknowledgements. This work was financially supported by the "Strategic Priority Research Program" of the Chinese Academy of Sciences (Grant No. XDB15010405), and Natural Science Foundation of China (Grant No. 41673020, 91747202, 41772380 and 41730857).

References:

Amiotte-Suchet, P., Probst, A. Probst, J.-L., Influence of acid rain on CO_2 consumption by rock weathering: local and global scales. Water Air Soil Pollut. 85, 1563-1568, 1995.

Amiotte-Suchet, P., Probst, J.-L. Ludwig, W., Worldwide distribution of continental rock lithology: implications for the atmospheric/soil CO_2 uptake by continental weathering and alkalinity river transport to the oceans. Global Biogeochem. Cycles 17, 1038-1052, 2003.

Bai, H., Song, L.S., Xia, W.P., Prospect analysis of hot dry rock (HDR) in Eastern part of Jiangxi province, Coal Geol. China 26, 41-44. (In Chinese), 2014.

Berner, R.A., Caldeira, K., The need for mass balance and feedback in the geochemical carbon cycle. Geology 25, 955-956, 1997.

Bluth, G.J.S., Kump, L.R., Lithological and climatological controls of river chemistry. Geochim. Cosmochim. Acta 58, 2341-2359, 1994.

Brantley, S.L., Lebedeva, M., Learning to read the chemistry of regolith to understand the Critical Zone. Annual Review of Earth and Planetary Sciences, 39: 387-416,

519 2011.
520 Calmels, D., Gaillardet, J., Brenot, A., France-Lanord, C., Sustained sulfide oxidation
521 by physical erosion processes in the Mackenzie River basin: climatic
522 perspectives. Geology 35, 1003-1006, 2007.
523 Calmels, D., Galy, A., Hovius, N., Bickle, M., West, A.J., Chen, M.-C., Chapman, H.,
524 Contribution of deep groundwater to the weathering budget in a rapidly eroding
525 mountain belt, Taiwan. Earth Planet. Sci. Lett. 303, 48-58, 2011.
526 Cerling, T.E., Solomon, D.K., Quade, J., Bownman, J.R., On the isotopic composition
527 of soil CO_2. Geochim. Cosmochim. Acta 55, 3403–3405, 1991.
528 Chen, Q., Shen, C., Sun, Y., Peng, S., Yi, W., Li Z., Jiang, M., Spatial and temporal
529 distribution of carbon isotopes in soil organic matter at the Dinghushan
530 Biosphere Reserve, South China. Plant and Soil, 273: 115–128, 2005.
531 Cheng, Y., Liu, Y., Huo, M., Sun, Q., Wang, H., Chen, Z., Bai, Y., Chemical
532 characteristics of precipitation at Nanping Mangdang Mountain in eastern China
533 during spring. J. Environ. Sci. 23, 1350-1358, 2011.
534 Chetelat, B., Liu, C., Zhao, Z., Wang, Q., Li, S., Li, J., Wang, B., Geochemistry of the
535 dissolved load of the Changjiang Basin rivers: anthropogenic impacts and
536 chemical weathering. Geochim. Cosmochim. Acta 72, 4254-4277, 2008.
537 Cui, J., Zhou, J., Peng, Y., He, Y., Yang, H., Mao, J., Atmospheric wet deposition of
538 nitrogen and sulfur to a typical red soil agroecosystem in Southeast China
539 during the ten-year monsoon seasons (2003-2012). Atmos. Environ. 82, 121-
540 129, 2014.

Das, A., Krishnaswami, S., Sarin, M.M., Pande, K., Chemical weathering in the Krishna Basin and Western Ghats of the Deccan Traps, India: Rates of basalt weathering and their controls. Geochim. Cosmochim. Acta 69(8), 2067-2084, 2005.

Dou, X., Deng, Q., Li, M., Wang, W., Zhang, Q., Cheng, X., Reforestation of Pinus massoniana alters soil organic carbon and nitrogen dynamics in eroded soil in south China. Ecological Engineering 52, 154-160, 2013.

Edmond, J.M., Palmer, M.R., Measures, C.I., Grant, B., Stallard, R.F., The fluvial geochemistry and denudation rate of the Guayana Shield in Venezuela, Colombia, and Brazil. Geochim. Cosmochim. Acta 59, 3301-3325, 1995.

Fan, B.L, Zhao, Z.Q., Tao, F.X., Liu, B.J., Tao, Z.H., Gao, S., He, M.Y., Characteristics of carbonate, evaporite and silicate weathering in Huanghe River basin: A comparison among the upstream, midstream and downstream. J. Asian Earth Sci. 96, 17-26, 2014.

Fang, Y., Wang, X., Zhu, F., Wu, Z., Li, J., Zhong, L., Chen, D., Yoh, M., Three-decade changes in chemical composition of precipitation in Guangzhou city, southern China: has precipitation recovered from acidification following sulphur dioxide emission control? Tellus B 65, 1-15, 2013.

Faure, G., Principles of Isotope Geology. Wiley, Toronto, pp. 492-493, 1986.

FJBGMR: Fujian Bureau of Geology and Mineral Resources, Regional Geology of Fujian Province. Geol. Publ. House, Beijing, p. 671 (in Chinese with English abstract), 1985.

563 Gaillardet, J., Dupré, B., Allègre, C.J., Négrel, P., Chemical and physical denudation
564 in the Amazon River basin. Chem. Geol. 142, 141-173, 1997.
565 Gaillardet, J., Dupré, B., Louvat, P., Allegre, C.J., Global silicate weathering and CO2
566 consumption rates deduced from the chemistry of large rivers. Chem. Geol. 159,
567 3-30, 1999.
568 Galy, A., France-Lanord, C., Weathering processes in the Ganges-Brahmaputra basin
569 and the riverine alkalinity budget. Chem. Geol. 159, 31-60, 1999.
570 Gandois, L., Perrin, A.-S., Probst, A., Impact of nitrogenous fertilizer-induced proton
571 release on cultivated soils with contrasting carbonate contents: A column
572 experiment. Geochim. Cosmochim. Acta 75, 1185-1198, 2011.
573 Gislason, S.R., Arnorsson, S., Armannsson, H., Chemical weathering of basalt in
574 southwest Iceland: effects of runoff, age of rocks and vegetative/glacial cover.
575 Am. J. Sci. 296, 837-907, 1996.
576 Han, G., Liu, C.Q., Water geochemistry controlled by carbonate dissolution: a study
577 of the river waters draining karst-dominated terrain, Guizhou Province, China.
578 Chem. Geol. 204, 1-21, 2004.
579 Han, Z.W., Ueda, H., Sakurai, T., Model study on acidifying wet deposition in East
580 Asia during wintertime. Atmos. Environ. 40, 2360-2373, 2006.
581 Hartmann, J., Jansen, N., Dürr, H.H., Kempe, S., Köhler, P., Global CO_2 consumption
582 by chemical weathering: what is the contribution of highly active weathering
583 regions? Global Planet. Change 69, 185-194, 2009.
584 Huang, K., Zhuang, G., Xu, C., Wang Y., Tang A., The chemistry of the severe acidic

precipitation in Shanghai, China. Atmos. Res. 89, 149-160, 2008.

Huh, Y.S., Chemical weathering and climate - a global experiment: a review. Geosci. J. 7, 277-288, 2003.

Hydrological data of river basins in Zhejiang, Fujian province and Taiwan region, Annual Hydrological Report P. R. China, 2010, Vol (7) (in Chinese)

Ji, H., Jiang, Y., Carbon flux and C, S isotopic characteristics of river waters from a karstic and a granitic terrain in the Yangtze River system. J. Asian Earth Sci. 57, 38-53, 2012.

Karim, A., Veizer, H.E., Weathering processes in the Indus River Basin: implication from riverine carbon, sulphur, oxygen and strontium isotopes. Chem. Geol. 170, 153-177, 2000.

Kendall, C., Tracing nitrogen sources and cycling in catchments. In: Kendall, C., & McDonnell, J.J., (Eds) Isotope Tracers in Catchment Hydrology. Elsevier, Amsterdam, 1998.

Kump, L.R., Brantley, S.L., Arthur, M.A., Chemical weathering, atmospheric CO_2 and climate. Ann. Rev. Earth Planet. Sci. 28, 611-667, 2000.

Larssen, T., Carmichael, G.R., Acid rain and acidification in China: the importance of base cation deposition. Environ. Poll. 110, 89-102, 2000.

Larssen, T., Lydersen, E., Tang, D., He, Y., Gao, J., Liu, H., Duan, L., Seip, H.M., Acid rain in China. Environ. Sci. Technol. 40, 418-425, 2006.

Lerman, A., Wu, L., CO_2 and sulfuric acid controls of weathering and river water composition. J. Geochem. Explor. 88, 427-430, 2006.

607 Lerman, A., Wu, L., Mackenzie, F.T., CO_2 and H_2SO_4 consumption in weathering and
608 material transport to the ocean, and their role in the global carbon balance. Mar.
609 Chem. 106, 326-350, 2007.
610 Li, S., Bush, R.T., Changing fluxes of carbon and other solutes from the Mekong
611 River. Sci. Rep. 5, 16005, 2015.
612 Li, S.Y., Lu, X.X., Bush, R.T., Chemical weathering and CO_2 consumption in the
613 Lower Mekong River. Sci. Total Environ. 472, 162-177, 2014.
614 Li, S.Y., Lu, X.X., He, M., Zhou, Y., Bei, R., Li, L., Zieglera, A.D., Major element
615 chemistry in the Upper Yangtze River: a case study of the Longchuanjiang
616 River. Geomorphology129, 29-42, 2011.
617 Li, S.Y., Xu, Z.F., Wang, H., Wang, J.H., Zhang, Q.F., Geochemistry of the upper Han
618 River basin, China. 3: anthropogenic inputs and chemical weathering to the
619 dissolved load. Chem. Geol. 264, 89-95, 2009.
620 Liu, B., Liu, C.-Q., Zhang, G., Zhao, Z.-Q., Li, S.-L., Hu, J., Ding, H., Lang, Y.-C.,
621 Li., X.-D., Chemical weathering under mid- to cool temperate and monsoon-
622 controlled climate: A study on water geochemistry of the Songhuajiang River
623 system, northeast China. Appl. Geochem. 31, 265-278, 2013.
624 Liu, L., Zhang, X., Wang, S., Zhang, W., Lu, X., Bulk sulfur (S) deposition in China.
625 Atmos. Environ., 135, 41-49, 2016.
626 Liu, W., Shi, C., Xu, Z., Zhao, T., Jiang, H., Liang, C., Zhang, X., Zhou, Li., Yu, C.,
627 Water geochemistry of the Qiantangjiang River, East China: Chemical
628 weathering and CO_2 consumption in a basin affected by severe acid deposition.

J.Asian Earth Sci., 127, 246-256, 2016.

Lu, C., Tian, H., Spatial and temporal patterns of nitrogen deposition in China: Synthesis of observational data. J. Geophys. Res. 112, D22S05, 2007.

Lu, Z., Zhang, Q., Streets, D.G., Sulfur dioxide and primary carbonaceous aerosol emissions in China and India, 1996e2010. Atmos. Chem. Phys. 11, 9839-9864, 2011.

Millot, R., Gaillardet, J., Dupré, B., Allègre, C.J., Northern latitude chemical weathering rates: clues from the Mackenzie River Basin, Canada. Geochim. Cosmochim. Acta 67, 1305-1329, 2003.

Millot, R., Gaillardet, J., Dupré, B., Allègre, C.J., The global control of silicate weathering rates and the coupling with physical erosion: new insights from rivers of the Canadian Shield. Earth Planet. Sci. Lett. 196, 83-98, 2002.

Ministry of Environmental Protection of China, 2009. China Environmental Quality Report 2008. China Environmental Sciences Press, Beijing. In Chinese.

Moon, S., Chamberlain, C.P., Hilley, G.E., New estimates of silicate weathering rates and their uncertainties in global rivers. Geochim. Cosmochim. Acta 134, 257-274, 2014.

Moon, S., Huh, Y., Qin, J., van Pho, N., Chemical weathering in the Hong (Red) River basin: Rates of silicate weathering and their controlling factors. Geochim. Cosmochim. Acta 71, 1411-1430, 2007.

Moon, S., Huh, Y., Zaitsev, A., Hydrochemistry of the Amur River: Weathering in a Northern Temperate Basin. Aquat. Geochem., 15, 497-527, 2009.

651 Mortatti, J., Probst, J.L., Silicate rock weathering and atmospheric/soil CO_2 uptake in
652 the Amazon basin estimated from river water geochemistry: seasonal and spatial
653 variations. Chem. Geol.197, 177-196, 2003.
654 Négrel, P., Allègre, C.J., Dupré, B., Lewin, E., Erosion sources determined by
655 inversion of major and trace element ratios and strontium isotopic ratios in river
656 water: the Congo Basin Case. Earth Planet. Sci. Lett. 120, 59-76, 1993.
657 Noh, H., Huh, Y., Qin, J., Ellis, A., Chemical weathering in the Three Rivers region of
658 Eastern Tibet. Geochim. Cosmochim. Acta 73, 1857-1877, 2009.
659 Oliva, P., Viers, J., Dupré B., Chemical weathering in granitic environments. Chem.
660 Geol. 202, 225-256, 2003.
661 Pan, Y.,Wang, Y., Tang, G., Wu, D., Spatial distribution and temporal variations of
662 atmospheric sulfur deposition in Northern China: insights into the potential
663 acidification risks. Atmos. Chem. Phys. 13, 1675-1688, 2013.
664 Pepin, E., Guyot, J.L., Armijos, E., Bazan, H., Fraizy, P., Moquet, J.S., Noriega, L.,
665 Lavado, W., Pombosa, R. Vauchel, P., Climatic control on eastern Andean
666 denudation rates (Central Cordillera from Ecuador to Bolivia). J. S. Am. Earth
667 Sci. 44, 85-93, 2013.
668 Perrin, A.-S., Probst, A., Probst, J.-L., Impact of nitrogenous fertilizers on carbonate
669 dissolution in small agricultural catchments: Implications for weathering CO_2
670 uptake at regional and global scales. Geochim, Cosmochim. Acta 72, 3105-
671 3123, 2008.
672 Probst, A., Gh'mari, A.El., Aubert, D., Fritz, B., McNutt, R., Strontium as a tracer of

673 weathering processes in a silicate catchment polluted by acid atmospheric
674 inputs, Strengbach, France. Chem. Geol. 170, 203-219, 2000.
675 Raymo, M.E., Ruddiman,W.F., Tectonic forcing of late Cenozoic climate. Nature 359,
676 117-122, 1992.
677 Raymond, P. A., Oh, N.H., Turner, R.E., Broussard, W., Anthropogenically enhanced
678 fluxes of water and carbon from the Mississippi River. Nature 451, 449-452,
679 2008.
680 Regnier, P., Friedlingstein, P., Ciais, P., Mackenzie, F.T.,…Thullner. M.,
681 Anthropogenic perturbation of the carbon fluxes from land to ocean. Nature
682 Geosci. 6, 597-607. 2013.
683 Reuss, J.O., Cosby, B.J., Wright, RF., Chemical processes governing soil and water
684 acidification. Nature 329, 27-32, 1987.
685 Roy, S., Gaillardet, J., Allègre, C.J., Geochemistry of dissolved and suspended loads
686 of the Seine river, France: anthropogenic impact, carbonate and silicate
687 weathering. Geochim. Cosmochim. Acta 63, 1277-1292, 1999.
688 Ryu, J.S., Lee, K.S., Chang, H.W., Shin, H.S., Chemical weathering of carbonates and
689 silicates in the Han River basin, South Korea. Chem. Geol. 247, 66-80, 2008.
690 Semhi, K., Amiotte Suchet, P., Clauer, N., Probst, J.-L., Impact of nitrogen fertilizers
691 on the natural weathering-erosion processes and fluvial transport in the Garonne
692 basin. Appl. Geochem. 15 (6), 865-874, 2000.
693 Shi, C., Chemical characteristics and weathering of rivers in the Coast of Southeast
694 China (PhD Thesis). Institute of Geology and Geophysics, Chinese academy of

695 sciences, Beijing, China. pp, 1-100 (in Chinese with English abstract), 2014.
696 Shin, W.-J., Ryu, J.-S., Park, Y., Lee, K.-S., Chemical weathering and associated CO_2
697 consumption in six major river basins, South Korea. Geomorphology 129, 334-
698 341, 2011.
699 Shu, L.S., Zhou, X.M., Deng, P., Wang, B., Jiang, S.Y., Yu, J.H., Zhao, X.X.,
700 Mesozoic tectonic evolution of the Southeast China Block: New insights from
701 basin analysis. J. Asian Earth Sci. 34(3), 376-391, 2009.
702 Spence, J., Telmer, K., The role of sulfur in chemical weathering and atmospheric
703 CO_2 fluxes: Evidence from major ions, $\delta^{13}C_{DIC}$, and$\delta^{34}S_{SO4}$ in rivers of the
704 Canadian Cordillera. Geochim. Cosmochim. Acta 69, 5441-5458, 2005.
705 Stallard, R.F., Edmond, J.M., Geochemistry of the Amazon. Precipitation chemistry
706 and the marine contribution to the dissolved load at the time of peak discharge.
707 J. Geophys. Res., 86, 9844-9858, 1981.
708 U.S. Nat. Res. Council Comm., Basic Research Opportunities in Earth Science.
709 Washington, DC: Nat. Acad. 154 pp., 2001.
710 Viers, J., Dupré, B., Braun, J.J., Freydier, R., Greenberg, S., Ngoupayou, J.N.,
711 Nkamdjou, L.S., Evidence for non-conservative behavior of chlorine in humid
712 tropical environments. Aquat. Geochem. 7, 127-154, 2001.
713 Vries, W.D., Reinds, G.J. Vel E., Intensive monitoring of forest ecosystems in Europe.
714 2-Atmospheric deposition and its impacts on soil solution chemistry. For. Ecol.
715 Manage. 174, 97-115, 2003.
716 Wang, T.J., Jin, L.S., Li, Z.K., Lam K.S., A modeling study on acid rain and

717 recommended emission control strategies in China. Atmos. Environ. 34, 4467-
718 4477, 2000.
719 West, A.J., Galy, A., Bickle, M., Tectonic and climatic controls on silicate weathering.
720 Earth Planet. Sci. Lett. 235, 211-228, 2005.
721 Wu, W., Zheng, H., Yang, J., Luo, C., Zhou, B., Chemical weathering, atmospheric
722 CO_2 consumption, and the controlling factors in a subtropical metamorphic-
723 hosted watershed. Chem. Geol. 356, 141-150, 2013.
724 Xiang, L., Study on Coupling between Water and Carbon of Artificial Forests
725 Communities in Subtropical Southern China. Master Dissertation, Institute of
726 Geographical Sciences and Natural Sources, Chinese Academy of Sciences,
727 China (in Chinese), 2006.
728 Xu, H., Bi, X-H., Feng, Y-C., Lin, F-M., Jiao, L., Hong, S-M., Liu, W-G., Zhang, X.-
729 Y., Chemical composition of precipitation and its sources in Hangzhou, China.
730 Environ. Monit. Assess. 183:581-592, 2011.
731 Xu, Y., Wang C.Y., Zhao T., Using detrital zircons from river sands to constrain major
732 tectono-thermal events of the Cathaysia Block, SE China. J. Asian Earth Sci.
733 124, 1-13, 2016.
734 Xu, Z., Liu, C.-Q., Chemical weathering in the upper reaches of Xijiang River
735 draining the Yunnan-Guizhou Plateau, Southwest China. Chem. Geol. 239, 83-
736 95, 2007.
737 Xu, Z., Liu, C.-Q., Water geochemistry of the Xijiang basin rivers, South China:
738 Chemical weathering and CO_2 consumption. Appl. Geochem. 25, 1603-1614,

2010.

Yoshimura, K., Nakao, S., Noto, M., Inokura, Y., Urata, K., Chen, M., Lin, P.W., Geochemical and stable isotope studies on natural water in the Taroko Gorge karst area, Taiwan - chemical weathering of carbonate rocks by deep source CO_2 and sulfuric acid. Chem. Geol. 177, 415–430, 2001.

Zhang, M., Wang, S., Wu, F., Yuan, X., Zhang, Y., Chemical compositions of wet precipitation and anthropogenic influences at a developing urban site in southeastern China. Atmos. Res. 84, 311-322, 2007a.

Zhang, S.R., Lu, X. X., Higgitt, D. L., Chen, C.T.A., Sun, H.-G., Han, J.T., Water chemistry of the Zhujiang (Pearl River): Natural processes and anthropogenic influences. J. Geophys. Res. 112, F01011, 2007b.

Zhao, W., An analysis on the changing trend of acid rain and its causes in Fujian Province. Fujian Geogr. 19, 1-5 (in Chinese), 2004.

Zhou, X.M., Li, W.X., Origin of Late Mesozoic igneous rocks in Southeastern China: Implications for lithosphere subduction and underplating of mafic magmas. Tectonophysics 326(3-4), 269-287, 2000.

Zhou, X.M., Sun, T., Shen, W.Z., et al., Petrogenesis of Mesozoic granitoids and volcanic rocks in South China: A response to tectonic evolution. Episodes 29(1), 26-33, 2006.

ZJBGMR: Zhejiang Bureau of Geology and Mineral Resources, Regional Geology of Zhejiang Province. Geol. Publ. House, Beijing, p. 617 (in Chinese with English abstract), 1989.

Table 1 Chemical and carbon isotopic compositions of river waters in the Southeast Coastal Rivers Basin (SECRB) of China.

Rivers	Sample number	Date (M/D/Y)	pH	T ℃	EC μs cm^{-1}	Na^+ μM	K^+ μM	Mg^{2+} μM	Ca^{2+} μM	F^- μM	Cl^- μM	NO_3^- μM	SO_4^{2-} μM	HCO_3^- μM	SiO_2 μM	TZ^+ μEq	TZ^- μEq	NICB %	$\delta^{13}C$ ‰	TDS mg l^{-1}
Qiantang*	1	07-8-10	7.42	28.78	190	347	197	106	473	12.0	303	62.6	147	1130	148	1703	1789	-5.0	-19.0	144
	2	07-9-10	7.60	23.84	146	87.5	204	80.9	496	11.7	75.2	124	121	907	156	1446	1348	6.7	-19.8	119
	3	07-9-10	7.37	27.83	308	555	233	208	698	41.8	312	223	437	1170	170	2601	2579	0.9	-17.8	204
	4	07-10-10	7.27	26.28	177	176	135	116	544	15.7	151	142	170	985	175	1632	1618	0.8	-19.3	135
	5	07-10-10	7.05	24.15	123	130	101	66.2	349	17.7	94.3	124	157	529	169	1061	1061	0.0	-18.7	91.2
	6	07-10-10	7.24	23.75	140	97.6	69.7	81.0	451	20.0	62.1	109	204	703	164	1231	1282	-4.2	-21.3	106.6
	7	07-11-10	7.40	23.23	107	92.5	70.5	68.3	327	14.9	74.9	104	147	486	156	954	960	-0.6	-21.0	82.2
	8	07-11-10	7.16	27.61	281	361	87.5	128	469	26.8	245	191	239	810	179	1642	1724	-5.0	-12.9	137.5
	9	07-11-10	7.02	26.48	140	275	120	60.7	319	36.2	199	150	180	437	236	1155	1146	0.8	-13.9	100.2
	10	07-12-10	7.05	24.24	99	205	114	58.3	285	14.6	191	114	132	305	278	1005	874	13.1	-20.9	85.4
	11	07-12-10	7.05	27.01	102	123	133	49.8	284	18.6	86.5	123	144	377	183	924	874	5.4	-19.2	79.4
	12	07-12-10	7.99	24.18	260	50.0	85.4	212	993	-	66.8	153	235	1822	172	2546	2512	1.4	-17.6	205.2
	13	07-12-10	7.86	24.59	231	43.5	88.4	189	859	-	55.1	97.6	169	1763	170	2228	2253	-1.1	-18.7	185.4
	14	07-12-10	7.69	22.66	131	44.1	81.0	113	458	-	19.1	95.2	107	920	143	1266	1248	1.4	-18.1	106.8
	15	07-12-10	7.65	24.48	106	61.1	98.3	87.9	335	-	37.2	68.3	112	663	164	1005	992	1.4	-18.6	87.3
	16	07-12-10	7.46	23.68	125	64.3	108	117	406	-	25.9	75.0	174	687	164	1218	1136	6.7	-20.0	98.8
	17	07-13-10	7.33	24.08	139	59.8	116	136	429	-	29.6	80.4	209	752	162	1305	1281	1.9	-20.8	108.1
	18	07-10-10	7.27	25.74	141	163	114	69.6	396	27.3	126	148	161	597	153	1209	1195	1.1	-21.0	101.0
Cao'e	19	07-16-10	7.17	22.27	108	212	86.3	69.4	183	5.1	151	148	114	384	216	803	912	-13.5	-21.2	79.1
	20	07-16-10	7.06	26.57	182	401	77.6	145	275	18.3	269	185	245	534	215	1318	1478	-12.2	-20.5	116.9
	21	07-16-10	7.14	27.26	171	333	91.3	164	362	18.1	224	194	207	658	225	1475	1490	-1.0	-20.9	123.3
	22	07-16-10	7.08	27.17	173	346	94.4	168	364	18.8	247	200	211	656	222	1506	1526	-1.3	-13.0	125.2
Ling	23	07-15-10	7.07	24.14	52	164	42.9	34.9	140	4.9	40.7	61.5	68.3	277	190	558	516	7.6	-12.8	52.1
	24	07-15-10	7.02	26.04	74	169	92.0	34.2	150	6.4	87.0	77.3	92.8	272	196	629	622	1.1	-20.8	59.5
	25	07-16-10	7.34	25.03	92	159	80.1	47.3	235	19.3	78.0	71.4	105	455	187	804	815	-1.4	-22.5	73.9
	26	07-16-10	7.40	26.75	113	216	77.8	57.1	249	20.2	133	90.0	115	494	196	905	946	-4.5	-12.7	82.8
	27	07-16-10	7.39	26	89	174	86.4	56.4	209	9.0	99.3	78.4	99.9	420	199	792	798	-0.8	-14.0	72.7
	28	07-15-10	6.79	22.33	75	159	82.7	44.1	143	-	107	61.8	83.4	306	144	616	641	-4.1	-21.1	56.5
	29	07-15-10	8.24	27.15	129	228	92.1	83.1	317	17.2	177	90.5	120	641	194	1120	1148	-2.5	-19.2	97.8
Ou	30	07-13-10	8.08	28.45	48	95.2	107	38.4	92.1	15.2	31.8	43.3	47.4	291	221	463	461	0.4	-21.7	50.6
	31	07-13-10	6.71	22.97	32	60.7	106	12.6	65.0	10.8	28.9	45.0	48.9	158	169	322	329	-2.2	-23.8	36.9
	32	07-13-10	7.18	27.59	73	107	127	36.2	175	4.3	57.1	111	92.0	283	210	655	634	3.2	-23.4	62.9
	33	07-13-10	6.94	24.2	44	76.9	112	20.0	99.1	10.9	27.9	63.1	58.6	249	184	427	457	-7.0	-22.5	47.5
	34	07-14-10	7.16	27.45	90	187	127	41.2	199.5	17.0	85.6	102	116	367	251	796	787	1.1	-22.4	76.5
	35	07-14-10	6.97	24.56	54	105	50.9	29.2	122	12.2	46.1	67.8	73.1	218	193	460	478	-4.1	-22.5	47.9
	36	07-14-10	6.82	21.12	31	76.4	133	12.7	74.5	7.7	20.7	36.8	49.1	192	162	383	348	9.3	-	39.5
	37	07-14-10	6.82	23.69	45	89.5	105	19.0	97.8	10.6	39.6	52.8	59.1	231	185	428	441	-3.0	-22.9	46.2
	38	07-15-10	6.92	24.69	37	100	89.3	21.1	49.7	1.7	36.9	45.5	52.7	153	202	331	341	-2.9	-	38.9
	39	07-15-10	6.90	23.86	35	92.2	92.0	19.8	61.4	1.9	43.9	47.9	55.5	139	193	347	342	1.4	-22.3	38.5
	40	07-15-10	7.09	25.56	47	117	112	25.7	83.4	8.0	52.4	63.1	57.4	232	193	447	462	-3.3	-22.5	48.1
	41	07-14-10	6.97	24.25	53	102	107	27.6	119	13.4	43.5	59.4	73.2	277	183	502	526	-4.9	-13.7	52.3

Feiyun	42	07-17-10	7.28	25.19	38	94.0	81.7	24.0	75.6	11.4	59.9	45.7	51.9	149	151	375	358	4.5	-	37.2
	43	07-17-10	7.08	25.61	46	101	79.9	33.9	93.4	4.6	66.2	55.1	52.8	223	151	435	450	-3.3	-23.7	43.5
Jiaoxi	44	07-17-10	7.52	26.92	47	116	81.5	25.2	92.0	4.1	73.3	80.3	25.0	226	151	432	430	0.5	-23.4	43.0
	45	07-17-10	7.45	27.46	61	152	90.2	34.2	119	-	136	59.8	53.5	238	184	548	542	1.2	-23.1	51.8
	46	07-18-10	6.90	27.66	53	127	88.1	33.4	94.4	7.0	123	93.1	30.4	209	177	471	486	-3.3	-14.4	47.4
Huotong	47	07-18-10	7.34	24	43	116	78.8	26.1	58.4	5.4	68.7	49.7	20.1	197	190	364	355	2.3	-22.8	39.6
Ao	48	07-19-10	7.24	31.44	124	294	121	102	209	24.3	204	73.6	52.0	717	370	1036	1100	-6.1	-19.4	105.4
	49	07-19-10	7.13	27.82	46	109	96.3	30.0	73.8	-	72.0	51.3	22.5	234	236	413	402	2.6	-	46.2
	50	07-18-10	6.98	28.65	53	140	88.4	40.8	100	3.0	82.9	58.6	20.9	294	233	511	477	6.6	-22.3	52.2
Min	51	07-27-10	7.11	28.4	42	116	92.0	40.5	119	18.0	43.9	35.5	26.0	382	182	526	513	2.4	-19.4	52.7
	52	07-27-10	7.17	30	51	102	97.9	41.7	107	4.6	29.4	45.3	35.0	350	221	496	495	0.2	-	53.3
	53	07-27-10	7.08	29.4	99	214	92.7	46.4	126	18.4	50.1	39.8	118	327	154	651	654	-0.4	-20.8	74.0
	54	07-27-10	7.06	29.1	44	107	99.6	28.1	114	16.4	18.7	36.4	44.3	305	265	491	449	8.5	-17.6	53.6
	55	07-27-10	7.42	29.4	57	139	93.7	49.8	113	3.1	67.1	56.3	26.6	384	236	558	561	-0.5	-16.4	58.6
	56	07-27-10	7.12	27.8	51	103	91.0	50.8	106	4.7	82.8	35.1	63.5	249	225	507	494	2.5	-	51.3
	57	07-27-10	7.08	27.5	40	125	45.0	36.8	107	12.1	43.6	44.5	29.3	288	211	457	435	5.0	-21.1	47.4
	58	07-27-10	6.99	27.2	52	121	98.0	42.4	115	16.7	87.1	36.6	70.9	277	228	535	542	-1.4	-11.4	55.3
	59	07-27-10	6.87	29	59	154	91.4	59.4	124	16.5	77.8	36.7	88.3	272	222	612	563	8.0	-20.3	57.2
	60	07-27-10	7.31	27.1	78	109	92.1	59.1	181	21.2	123	37.5	78.4	355	202	682	672	1.4	-18.7	63.1
	61	07-27-10	7.22	27.8	37	122	83.3	52.8	142	17.4	111	37.3	80.4	288	221	596	597	-0.2	-22.3	58.1
	62	07-27-10	7.16	28.1	58	104	83.3	59.3	163	24.0	34.6	34.5	118	294	214	632	599	5.2	-13.4	59.5
	63	07-27-10	7.26	28.3	87	139	86.1	60.9	191	14.8	48.0	93.0	109	347	226	729	707	3.0	-21.4	68.6
	64	07-27-10	7.00	28.8	87	127	93.1	58.7	195	6.6	59.8	81.1	60.9	480	232	729	743	-2.0	-11.0	74.0
	65	07-28-10	6.97	27.9	37	163	82.1	52.2	140	20.2	53.1	60.0	106	306	221	630	632	-0.2	-	61.9
	66	07-13-10	7.07	27.96	59	91.9	110	40.0	127	24.8	62.0	79.3	62.3	249	228	535	515	3.8	-	54.8
	67	07-28-10	7.12	29.7	38	108	93.4	45.9	133	12.4	48.3	34.0	56.6	368	220	560	564	-0.7	-	57.7
	68	07-27-10	7.03	29.9	62	128	96.7	57.6	148	23.3	81.6	36.8	74.1	374	203	635	641	-0.9	-12.4	61.7
	69	07-27-10	7.01	28.8	60	102	89.1	73.6	138	9.6	50.6	74.1	32.7	417	233	615	607	1.3	-21.0	62.3
	70	07-27-10	7.06	26.5	37	93.5	93.1	34.7	87.3	-	26.6	34.8	37.1	312	222	431	448	-3.9	-13.1	49.1
	71	07-27-10	7.09	26.5	25	62.6	92.7	27.0	61.5	4.7	21.5	18.6	43.4	191	154	332	318	4.2	-16.0	35.3
	72	07-28-10	7.07	30.1	39	76.3	87.9	35.1	87.6	7.4	43.1	36.6	35.5	266	175	409	416	-1.7	-19.4	43.5
	73	07-27-10	7.01	28.7	47	84.9	95.4	56.7	106	12.7	51.8	49.2	57.2	315	211	506	531	-4.8	-	53.8
	74	07-27-10	6.85	28.7	50	93.6	85.9	52.4	107	14.1	62.8	57.5	57.0	252	217	498	487	2.2	-19.9	50.9
	75	07-27-10	7.11	29.7	69	117	85.2	73.4	159	7.6	63.7	75.2	47.4	418	230	666	652	2.2	-22.2	65.0
	76	07-28-10	6.93	28.9	59	112	88.0	61.8	122	6.0	57.4	89.3	42.0	349	224	568	580	-2.2	-22.0	58.8
	77	07-21-10	7.76	32.4	51.2	163	85.5	52.8	151	20.2	55.3	70.3	78.6	372	175	656	655	0.3	-12.5	61.8
	78	07-28-10	7.29	26.8	106	129	75.3	84.0	321	24.0	56.2	41.0	166	599	202	1013	1028	-1.4	-16.3	90.3
	79	07-21-10	7.09	26.96	56	112	87.6	37.1	129	4.5	51.5	44.9	61.9	327	276	531	547	-2.9	-22.2	59.1
	80	07-21-10	7.64	33.37	83	114	96.2	60.6	151	16.7	53.0	40.6	102	371	242	633	670	-5.8	-12.8	66.2
	81	07-21-10	7.83	31.27	65	131	102	52.7	141	16.1	45.3	49.7	91.8	324	239	620	603	2.8	-13.4	61.8
	82	07-21-10	6.84	28.35	66	132	101	52.5	141	5.8	63.8	54.1	91.6	304	243	621	606	2.5	-22.7	61.5
	83	07-21-10	7.42	30.7	98	217	113	59.2	210	18.4	98.7	63.5	84.7	496	320	868	827	4.6	-18.9	84.5
	84	07-27-10	7.26	26.3	46	104	102	29.7	121	3.6	55.2	51.9	55.5	294	193	507	512	-0.9	-21.6	51.9
	85	07-27-10	7.07	25.4	30	73.3	99.2	19.6	78.8	-	22.9	40.0	49.2	203	170	369	365	1.3	-21.1	39.8
	86	07-27-10	7.50	27.3	45	102	102	26.5	114	2.4	35.1	39.7	57.2	260	217	484	449	7.3	-15.7	49.6
	87	07-27-10	7.47	26.9	51	141	100	43.6	109	7.9	79.7	42.4	57.7	311	217	547	548	-0.3	-20.1	55.6

	88	07-19-10	7.99	31.74	63	167	96.5	33.5	115	8.0	105	35.5	38.1	331	218	561	548	2.3	-13.5	55.9
	89	07-21-10	6.77	28.19	65	132	93.6	56.0	145	15.6	60.6	78.8	75.4	333	243	627	624	0.5	-22.6	63.3
Jin	90	07-27-10	7.36	25.8	128	126	94.8	88.9	406	22.9	51.4	39.4	229	595	208	1211	1143	5.6	-20.7	100
	91	07-27-10	7.40	26.9	123	143	103	82.7	347	21.0	83.5	203	182	463	226	1105	1115	-0.9	-21.3	98.4
	92	07-27-10	7.00	27.4	88	170	98.8	56.8	205	7.2	137	117	106	327	205	793	792	0.1	-22.5	71.8
	93	07-27-10	7.32	28.7	73	201	116	87.1	318	20.0	93.5	41.5	189	508	267	1128	1020	9.6	-21.7	95.3
Jiulong	94	07-30-10	6.50	23.47	29	72.3	92.4	22.8	59.8	12.4	25.1	27.0	50.0	189	213	330	341	-3.4	-18.1	40.1
	95	07-30-10	7.06	29.35	120	136	96.9	106	339	5.1	67.7	66.3	249	469	202	1124	1100	2.1	-20.8	94.2
	96	07-30-10	7.45	27.6	104	79.5	97.5	106	363	14.4	70.7	50.0	99.9	729	184	1116	1049	6.0	-18.9	93.7
	97	07-31-10	7.36	26.59	139	140	100	142	432	15.5	79.6	78.3	274	573	196	1388	1278	8.0	-19.7	108.8
	98	07-31-10	7.72	26.18	88	77.6	96.2	69.0	313	19.9	39.7	34.6	63.8	731	251	938	933	0.5	-18.4	89.4
	99	07-30-10	7.43	26.96	119	200	93.8	100.2	298	19.9	122	80.5	225	387	202	1091	1040	4.7	-20.5	89.5
	100	07-28-10	7.41	26.66	112	173	97.9	94.4	286	46.1	118	152	201	364	207	1033	1036	-0.3	-20.9	92.2
	101	07-29-10	7.16	29.35	82	151	110	55.4	178	4.9	71.2	170	53.2	385	305	727	732	-0.7	-21.2	76.1
	102	07-29-10	7.10	28.9	100	222	98.3	49.4	249	3.6	126	157	52.7	532	303	917	920	-0.3	-21.7	90.0
	103	07-28-10	7.20	31.15	138	339	111	81.2	277	9.2	280	285	88.6	515	317	1165	1256	-7.8	-19.0	112
	104	07-28-10	7.16	27.09	101	261	95.8	81.7	235	40.3	173	80.1	174	291	136	990	892	9.9	-24.3	75.4
Zhang	105	07-28-10	8.08	30.6	93	195	96.1	61.1	167	16.8	157	193	55.2	281	288	748	741	0.9	-21.5	73.8
Dongxi	106	07-28-10	7.20	30.9	78	263	99.0	41.5	115	14.5	238	65.3	30.0	283	309	675	646	4.4	-20.8	66.7
Huangang	107	07-28-10	7.40	30.5	99	253	85.6	53.0	154	7.7	190	63.5	56.4	460	278	754	827	-9.6	-20.0	77.4
Han	108	07-31-10	7.31	27.1	68	136	61.5	45.2	195	16.1	37.7	45.3	93.7	345	218	678	615	9.2	-21.9	62.0
	109	07-30-10	7.38	26.94	88	116	103	63.6	265	6.4	53.4	72.2	84.9	584	244	876	879	-0.4	-20.4	83.7
	110	07-30-10	6.66	25.55	71	114	96.2	47.6	168	8.0	56.9	54.6	143	230	203	642	628	2.2	-17.9	59.7
	111	07-30-10	6.66	27.76	83	135	104	63.8	203	8.6	54.5	74.9	173	302	336	774	777	-0.4	-20.6	78.7
	112	07-30-10	7.31	30.81	56	168	74.0	39.1	118	13.5	62.9	44.4	81.4	237	245	556	507	8.8	-21.4	54.6
	113	07-31-10	7.28	28.73	98	137	99.3	85.6	270	9.2	88.8	59.1	118	565	233	948	949	-0.1	-19.7	86.6
	114	07-31-10	7.27	31.42	123	193	105	98.2	319	20.7	120	102	157	570	229	1132	1107	2.2	-19.7	98.2
	115	07-30-10	7.43	29.89	85	115	97.5	65.5	244	6.5	46.5	58.6	103	511	251	832	822	1.1	-20.8	79.3
	116	07-31-10	7.61	30.98	99	123	104	85.9	264	5.6	58.8	90.9	108	588	98	926	952	-2.9	-20.0	79.4
	117	07-31-10	7.31	29.96	93	151	103	78.1	250	15.4	68.0	99.1	173	379	233	909	891	1.9	-21.9	81.8
	118	07-31-10	7.35	28.4	2	233	84.2	101	323	12.8	84.0	101	203	460	229	1165	1051	9.8	-21.1	94.7
	119	07-31-10	7.67	30.38	93	136	87.8	73.6	231	16.4	64.6	94.4	184	382	226	834	909	-9.1	-20.8	80.5
Rong	120	07-30-10	7.57	31.83	68	193	79.1	50.3	146	16.4	192	84.0	31.5	344	309	664	683	-2.8	-20.3	65.8
	121	07-30-10	6.96	30.62	94	509	103	56.1	213	15.9	511	78.5	82.3	379	222	1150	1133	1.5	-20.0	94.4

TZ^+ is the total cationic charge; TZ^- is the total anionic charge; NICB is the normalized inorganic charge balance and TDS is the total dissolved solid. *data of major ion composition from the previous work by Liu et al. 2016.

Table 2 Chemical compositions of precipitation at different sites located within the studied area (in μmol l^{-1} and molar ratio).

Province	Location	pH	F^-	Cl^-	NO_3^-	SO_4^{2-}	NH_4^+	K^+	Na^+	Ca^{2+}	Mg^{2+}	NO_3/Cl	SO_4/Cl	K/Cl	Na/Cl	Ca/Cl	Mg/Cl	Reference
Zhejiang	Hangzhou	4.5	5.76	13.9	38.4	55	79.9	4.18	12.2	26	3.53	2.76	3.96	0.3	0.88	1.87	0.25	Xu et al., 2011
	Jinhua	4.54	9.05	8.51	31.2	47.6	81.1	4.73	6.27	24	1.73	3.67	5.59	0.56	0.74	2.81	0.2	Zhang et al., 2007
Fujian	Nanping	4.81	0.8	5.8	26.6	18.3	38	4.9	5.4	12.9	2.7	4.59	3.16	0.84	0.93	2.22	0.47	Cheng et al., 2011
	Fuzhou		5.26	21.4	24.9	48.5	78.1	4.1	2.61	32.7	1.25	1.16	2.26	0.19	0.12	1.53	0.06	Zhao, 2004
	Xiamen	4.57	15.3	23.7	22.1	31.3	37.7	3.58	36.1	21.5	4.94	0.93	1.32	0.15	1.52	0.91	0.21	Zhao, 2004
Average												2.62	3.26	0.41	0.84	1.87	0.24	

Table 3 Contribution of each reservoir, fluxes, chemical weathering and associated CO_2 consumption rates for the major rivers and their main tributaries in the SECRB.

Major river	Tributaries	Location	Discharge	Area	Runoff	Contribution (%)				Fluxes (10^6 ton a^{-1})		Weathering rate (ton $km^{-2}a^{-1}$)				CO_2 consumption rate (10^3 mol km^{-2} a^{-1})			
			10^9 m^3a^{-1}	10^3 km^2	mm a^{-1}	Rain	Anth.	Sil.	Carb.	SWF	CWF	Cat_{sil}[a]	SWR[b]	CWR[b]	TWR[b]	CSW[c]	CCW[c]	SSW[d]	SSW[e]
Qiantang		Fuyang	43.81	38.32	1143	9	14	23	54	0.66	1.74	6.8	17.3	45.3	62.6	223	459	195	184
	Fenshui	Tonglu	2.726	3.100	879	7	14	18	62	0.05	0.16	5.5	14.7	52.1	66.8	167	530	152	146
Cao'e		Huashan	2.610	3.043	858	7	23	26	44	0.06	0.11	6.8	18.2	35.4	53.5	269	369	240	229
Ling		Linhai	5.400	6.613	817	9	22	24	45	0.09	0.17	4.7	14.2	26.1	40.3	167	267	143	133
	Yonganxi	Baizhiao	3.184	2.475	1286	14	15	50	21	0.06	0.03	9.1	24.2	11.7	35.9	350	119	255	216
	Shifengxi	Shaduan	1.731	1.482	1168	11	19	35	36	0.03	0.04	7.6	21.4	24.5	45.9	304	249	249	227
Ou		Hecheng	20.65	13.45	1536	20	6	56	18	0.36	0.13	10.1	26.9	9.9	36.9	360	101	228	174
	Haoxi	Huangdu	1.809	1.270	1447	16	8	46	30	0.04	0.02	9.9	27.9	19.0	46.9	336	192	246	210
	Xiaoxi	Jupu	5.116	3.336	1534	23	0	74	4	0.09	0.01	11.4	26.4	1.8	28.2	391	18	202	125
	Nanxi	Yongjiashi	1.799	1.273	1413	21	9	63	7	0.03	0.00	10.0	26.3	3.3	29.6	360	34	200	135
Huotong		Yangzhong	3.470	2.082	1667	22	18	54	5	0.06	0.00	8.3	27.3	2.1	29.4	305	24	129	59
Ao		Lianjiang	2.770	3.170	874	17	17	48	17	0.05	0.02	5.1	17.3	5.4	22.7	188	56	122	95
Min		Zhuqi	84.59	54.50	1552	15	10	48	27	1.80	0.94	10.3	33.0	17.3	50.2	390	180	292	252
	Futun	Yangkou	22.53	12.67	1778	15	14	49	22	0.45	0.21	12.0	35.8	16.2	52.0	460	171	336	286
	Shaxi	Shaxian	12.87	9.922	1297	13	9	42	36	0.26	0.21	8.4	26.5	21.7	48.1	315	222	249	223
	Jianxi	Qilijie	24.91	14.79	1685	16	10	45	29	0.48	0.26	9.6	32.2	17.4	49.6	350	185	250	210
	Youxi	Youxi	5.237	4.450	1177	15	8	46	31	0.11	0.07	7.4	24.5	15.0	39.5	272	156	205	178
	Dazhangxi	Yongtai	4.205	4.034	1042	15	21	47	17	0.08	0.03	6.6	20.2	7.1	27.4	242	73	163	131
Jin	Xixi	Anxi	3.004	2.466	1218	9	10	29	52	0.06	0.10	7.9	24.4	42.2	66.6	284	430	247	232
	Dongxi	Honglai	2.236	1.704	1312	12	22	28	38	0.04	0.04	6.8	22.9	25.6	48.5	226	263	178	158
Jiulong		Punan	10.20	8.49	1201	13	14	28	45	0.19	0.29	7.3	22.2	34.0	56.2	263	351	209	188
	Xi'xi	zhengdian	4.080	3.420	1193	10	32	25	33	0.10	0.11	8.0	30.7	30.9	61.6	288	317	227	203
Zhang		Yunxiao	1.011	1.038	974	16	25	29	29	0.02	0.01	5.1	21.9	14.1	36.0	174	146	114	90
Dongxi		Zhao'an	1.176	0.955	1231	16	41	26	17	0.03	0.01	5.8	28.7	10.2	38.9	187	107	93	55
Huanggang		Raoping	1.637	1.621	1010	15	30	34	21	0.04	0.02	6.0	22.8	11.1	33.9	227	115	145	112
Han		Chao'an	24.75	29.08	851	16	7	38	39	0.49	0.50	5.4	17.0	17.0	34.0	208	176	156	135

Ding	Xikou	11.14	9.228	1207	17	6	46	32	0.31	0.18	9.0	33.3	19.1	52.4	341	196	249	212
Mei	Hengshan	10.29	12.95	794	12	13	31	44	0.21	0.32	5.7	16.6	24.5	41.1	212	252	173	157
Whole SECRB		207	167	1240					3.95	4.09	7.8	23.7	24.5	48.1	287	251	218	191

[a] Cat_{sil} are calculated based on the sum of cations from silicate weathering.

[b] SWR, CWR and TWR represent silicate weathering rates (assuming all dissolved silica is derived from silicate weathering), carbonate weathering rates and total weathering rates, respectively.

[c] CO_2 consumption rate with assumption that all the protons involved in the weathering reaction are provided by carbonic acid.

[d] Estimated CO_2 consumption rate by silicate weathering when H_2SO_4 from acid precipitation is taken into account.

[e] Estimated CO_2 consumption rate by silicate weathering when H_2SO_4 and HNO_3 from acid precipitation is taken into account.

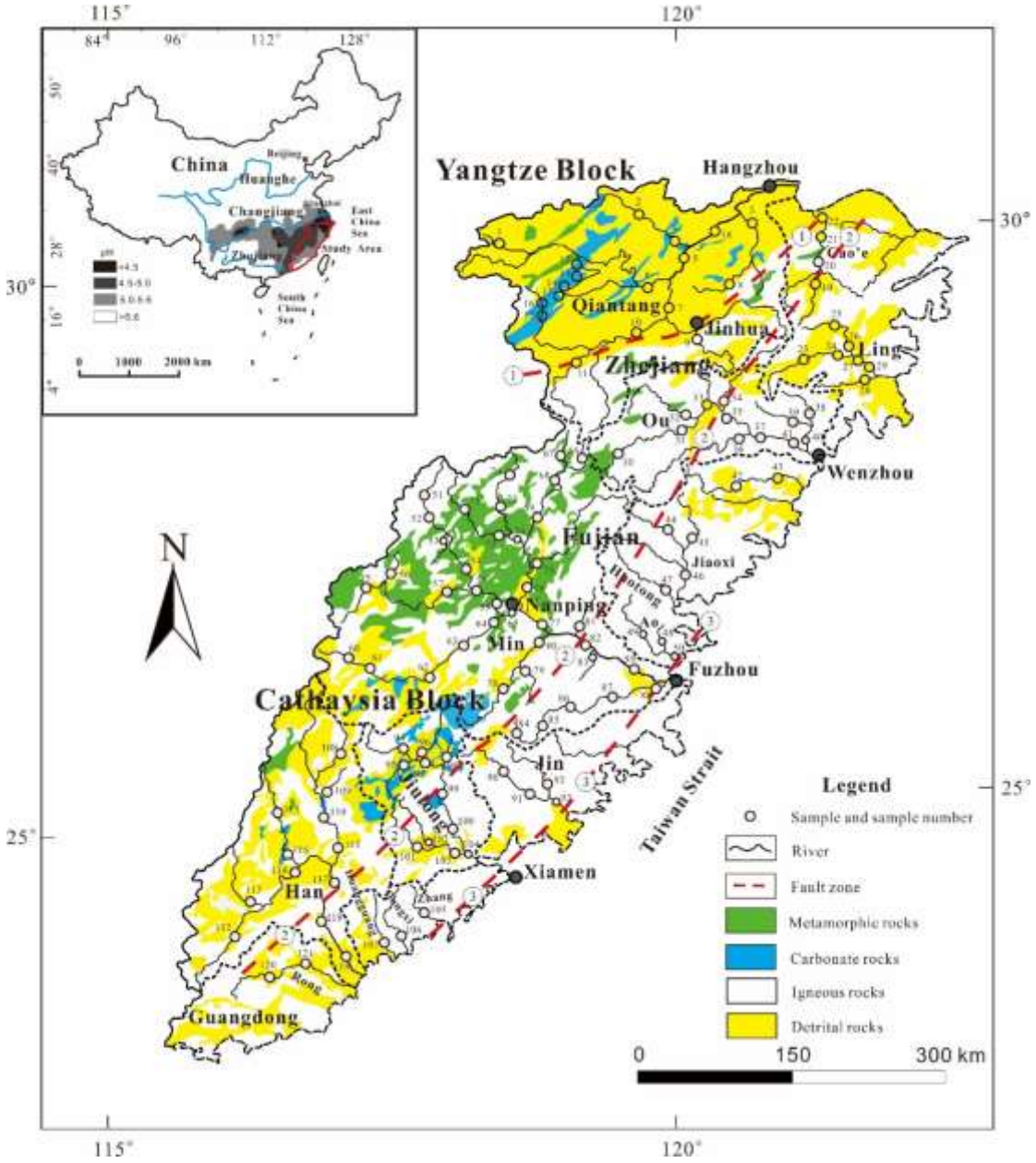

Fig. 1. Sketch map showing the lithology, sampling locations, and sample number of the SECRs drainage basin, and regional rain water pH ranges are shown in the sketch map at the upper-left. (modified from Zhou and Li, 2000; Shu et al., 2009; Xu et al., 2016, rain water acidity distribution of China mainland is from State Environmental Protection Administration of China). ①Shaoxing-Jiangshan fault zone; ②Zhenghe-Dapu fault zone; ③Changle-Nanao fault zone. The figure was created by CorelDraw software version 17.1.

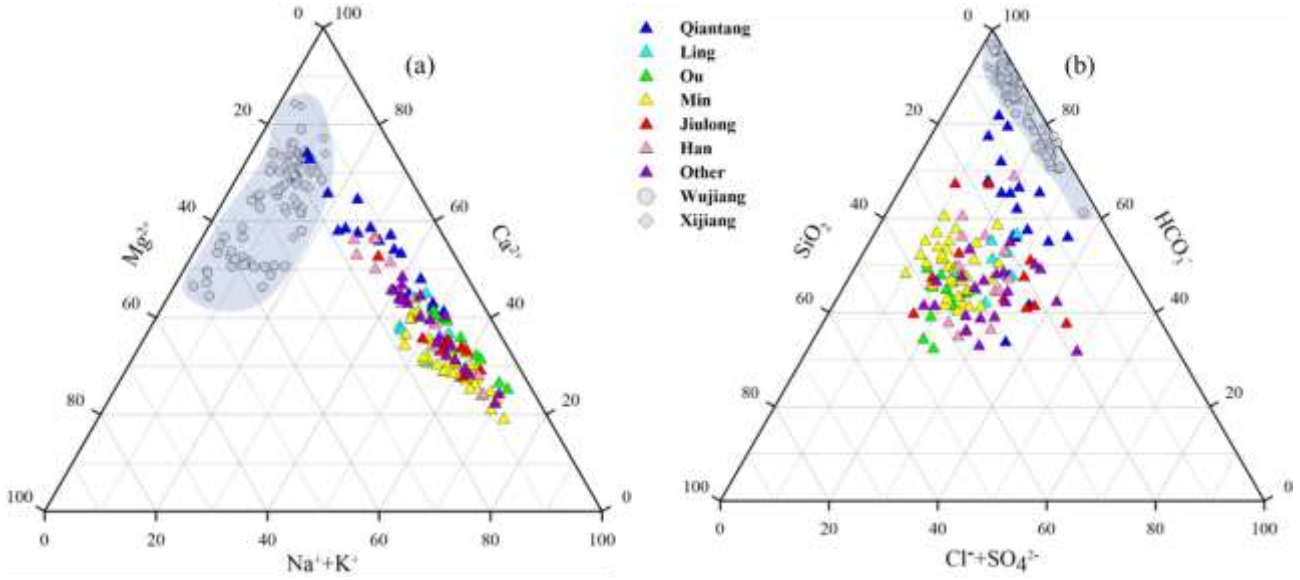

Fig. 2. Ternary diagrams showing cations (a), anions and dissolved SiO_2 (b) compositions of river waters in the SECRB. Chemical compositions from case studies of rivers draining carbonate rocks (the Wujiang and the Xijiang) are also shown for comparison (data from Han and Liu 2004; Xu and Liu 2007, 2010)

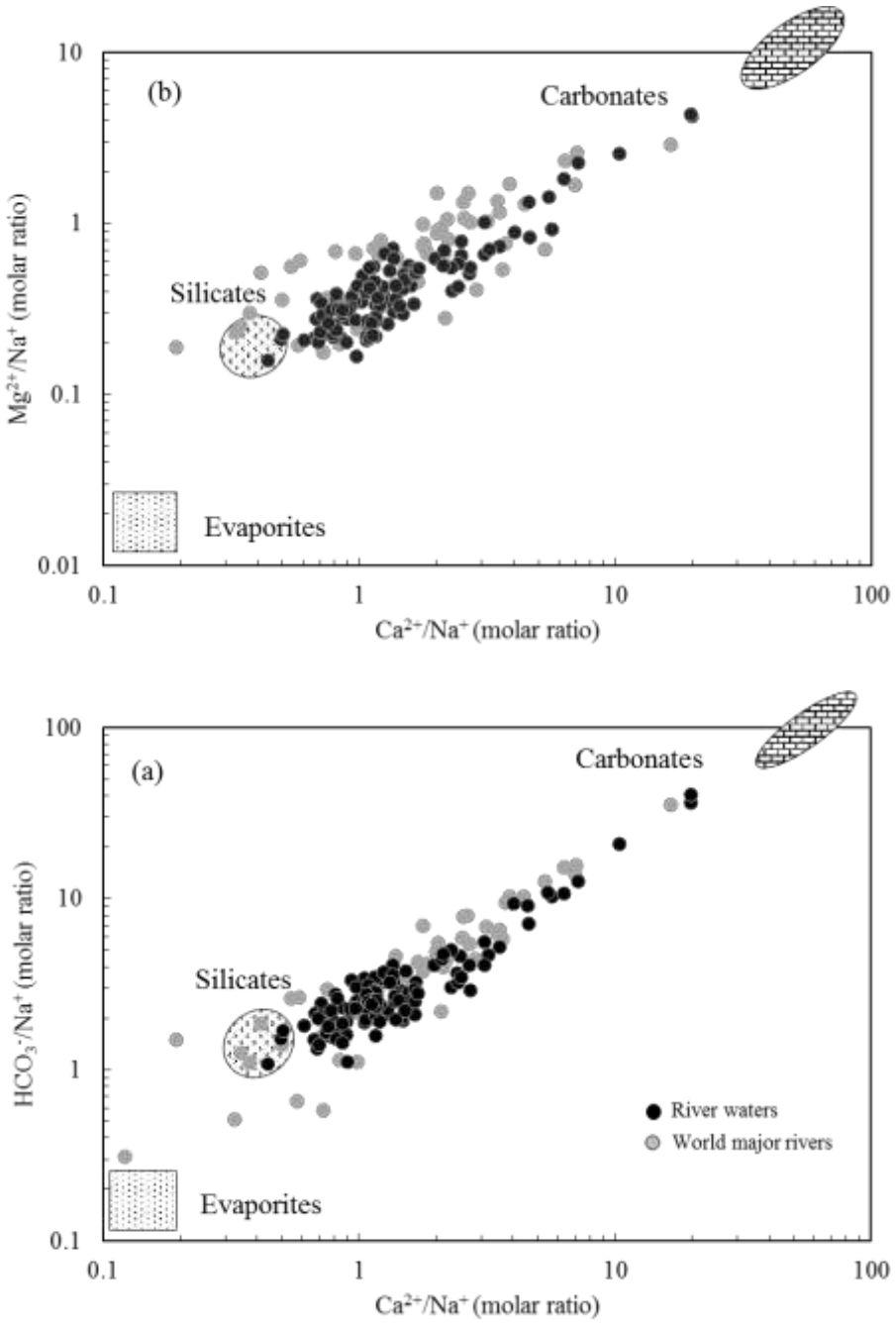

Fig. 3. Mixing diagrams using Na-normalized molar ratios: HCO_3^-/Na^+ *vs.* Ca^{2+}/Na^+ (a) and Mg^{2+}/Na^+ *vs.* Ca^{2+}/Na^+ (b) for the SECRB. The samples mainly cluster on a mixing line between silicate and carbonate end-members. Data for world major rivers are also plotted (data from Gaillardet et al. 1999).

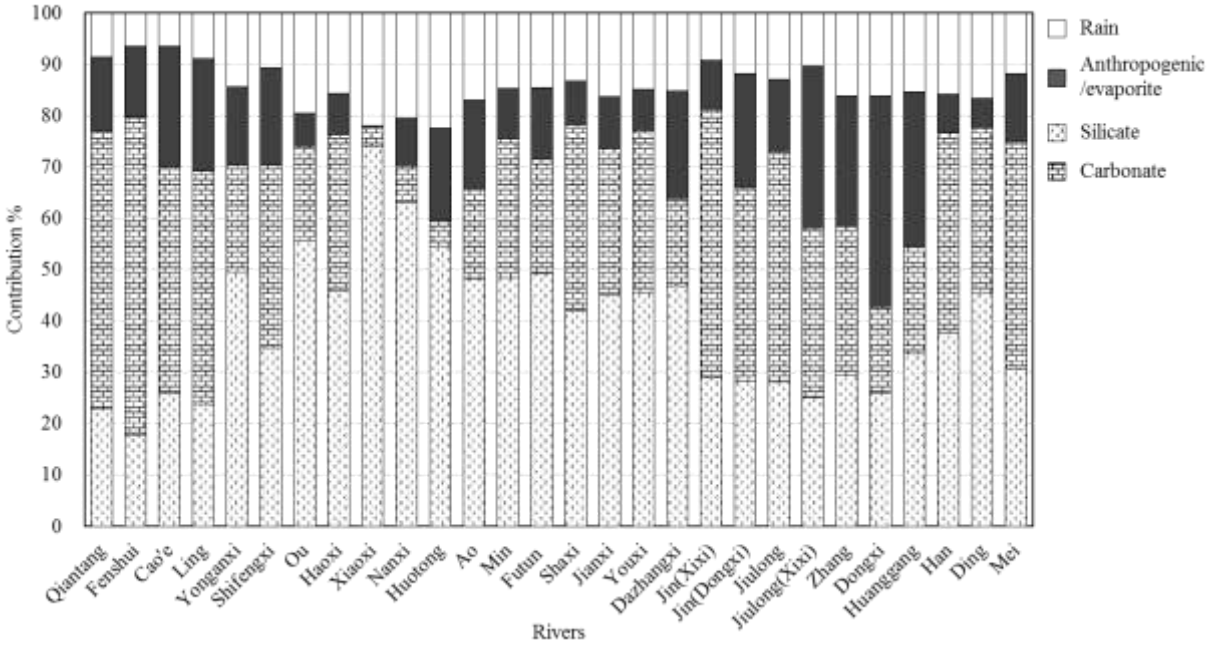

Fig. 4. Calculated contributions (in %) from the different reservoirs to the total cationic load for major rivers and their main tributaries in the SECRB. The cationic load is equal to the sum of Na^+, K^+, Ca^{2+} and Mg^{2+} from the different reservoirs.

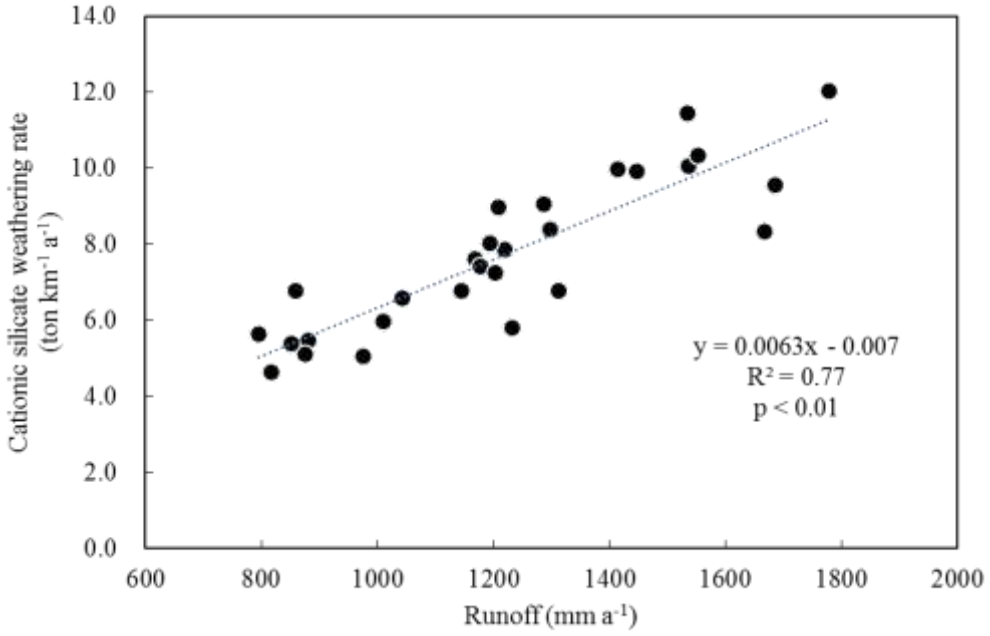

Fig. 5. Plots of the cationic-silicate weathering rate (Cat_{sil}) vs. runoff for the SECRB, showing that the silicate weathering rates is controlled by the runoff.

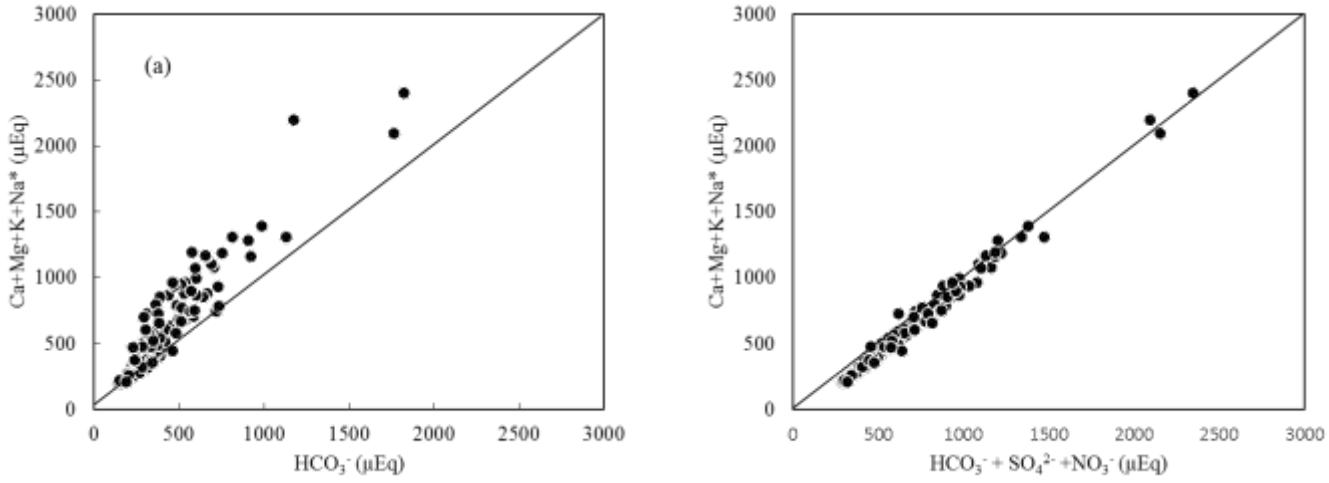

Fig. 6. Plots of total cations derived from carbonate and silicate weathering *vs.* HCO_3^- (a) and $HCO_3^-+SO_4^{2-}+NO_3^-$ (b) for river waters in the SECRB.

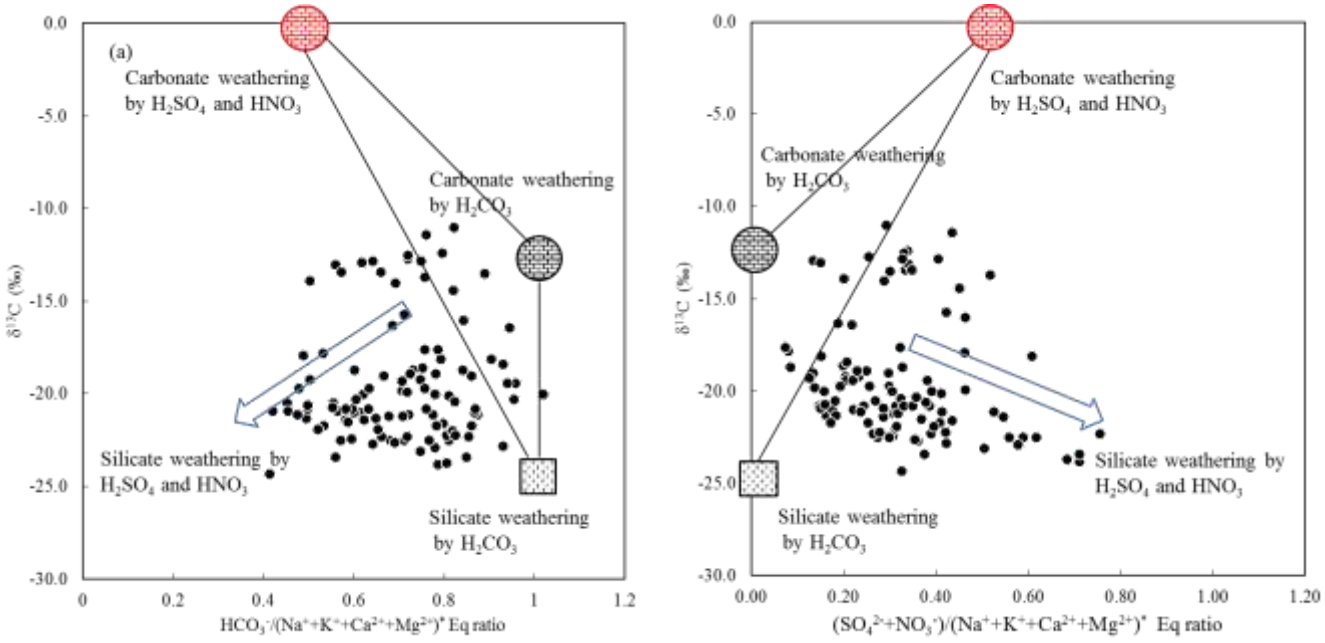

Fig. 7. $\delta^{13}C_{DIC}$ *vs.* $HCO_3^-/(Na^++K^++Ca^{2+}+Mg^{2+})^*$ (a) and $(SO_4^{2-}+NO_3^-)/(Na^++K^++Ca^{2+}+Mg^{2+})^*$ equivalent ratio (b) in river waters draining the SECRB (* means corrected for atmospheric and anthropogenic inputs). The plot show that most waters deviate from the three endmember mixing area (carbonate weathering by carbonic acid and sulfuric acid and silicate weathering by carbonic acid), illustrating the effect of sulfuric and nitric acid on silicate weathering.